J. Phys. D: Appl. Phys. **25** (1992) 563–586. Printed in the UK

REVIEW ARTICLE

Laser diode pumped solid state lasers

D W Hughes and J R M Barr

Department of Physics and Optoelectronics Research Centre, Southampton University, Southampton SO9 5NH, UK

Received 25 October 1991

Abstract. Solid state lasers have undergone a renaissance since the development of reliable and cheap laser diodes which can be used as pump sources. The result is compact, efficient laser sources which are attractive for a wide range of applications. This review summarizes the properties of laser diodes which are advantageous for pumping solid state lasers and describes the diverse laser materials and configurations of solid state lasers reported in the literature.

1. Introduction

Laser diode pumped solid state lasers (LDPSSLs) have, over the last five or six years, become very important in the laboratory and are beginning to make an impact in the market place. This growth in interest can be traced directly to the production of semiconductor laser diodes (LDs) in large quantities with well defined characteristics—particularly with regard to wavelength stability, efficiency and lifetime. The large volume production runs of LDs that are now possible have significantly reduced the unit cost of delivered power from semiconductor LDs. LDs are available with a range of wavelengths, which makes them ideal sources to pump solid state lasers, thus yielding a device which is sufficiently compact to warrant the name miniature and which can achieve very large conversion efficiencies from electrical to optical power.

This review is arranged in the following manner: section 2 describes the historical development of LDPSSLs; section 3 introduces LDs in sufficient detail for the purposes of this review; section 4 discusses the various pumping schemes that have been utilized in LDPSSLs; section 5 summarizes recent progress in a variety of LDPSSLs; section 6 covers the various reports of short pulse generation from modelocked LDPSSLs; section 7 outlines the techniques used to produce single frequency generation from a LDPSSL; and finally section 8 summarizes the material of the review.

Before proceeding with the text of the review the properties of LDPSSLs that are novel and make the LDPSSL a fertile field for research will be outlined. These points will be fully discussed in the main parts of the review but a list which the reader can keep in mind may help to emphasize the main points and to introduce the concepts that characterize LDPSSLs.

(1) The complete diode pumped solid state laser system is efficient. Electrical to optical conversion efficiencies of 15.8% have been obtained [1].

(2) Lifetimes of the LD are long, particularly when compared with traditional pumping schemes. Typically a continuous wave (CW) LD may be expected to have a lifetime well in excess of 100 h continuous operation. In fact the lifetime for many commercial devices are too long to measure directly and are extrapolated from accelerated ageing tests. A value of 40 000 h for a 50% increase in current to maintain a specified output power has been measured for a 500 mW array [2].

(3) The pump source is selective and only pumps a single absorption band of the active ion, in contrast to flashlamps which pump over most of the visible spectrum. This reduces the heat loading which results from the difference in wavelength between the pump laser and the lasing wavelength. Consequently thermal effects such as thermal birefringence, thermal lensing and thermal damage are significantly reduced. The overall optical to optical conversion efficiency (i.e. from pump power to useful output power) of LDPSSLs may be in the region of 20–60%.

(4) The output beam quality of a LDPSSL can closely approximate to a TEM_{00} mode which is a vast improvement over the properties of the LD itself. LDs typically have a non-circular beam profile due to the dimensions of the emitting region. This point is elaborated further in section 3.

(5) The LD is not a suitable device for high-power peak power applications. The short recombination lifetime of holes and electrons (1 ns) prohibits significant energy storage. The upper level lifetime of LD pumpable solid state lasers normally exceeds 200 μs indicating that these systems are suitable for Q-switching. The small area of the emission region and the low intensity required for catastrophic optical damage ensures that LDs are effectively low-power devices.

(6) The LD is a very quiet pump source with good amplitude stability. To a good degree the LDPSSL is also a quiet source. As a consequence of this some small

0022-3727/92/040563 + 24 $04.50

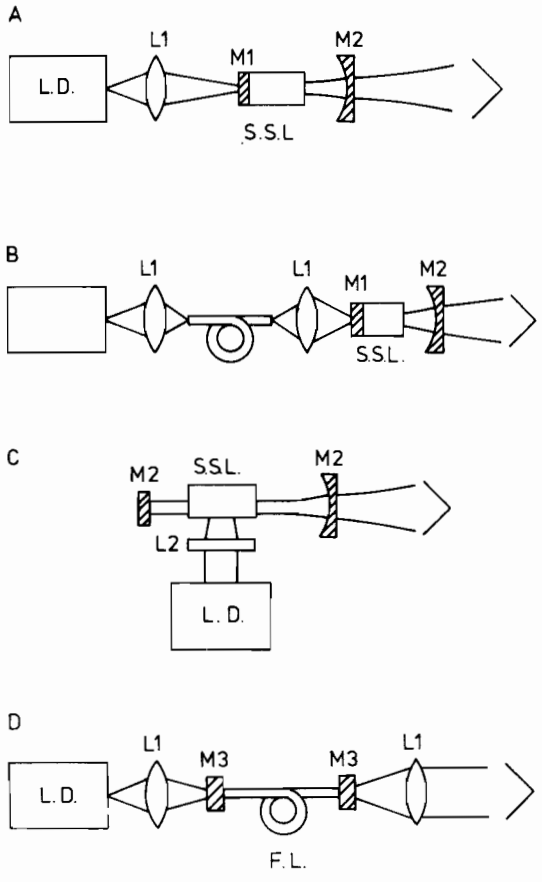

Figure 1. An illustration of a number of LD pumping geometries. The following notation is used: LD, laser diode; M1, mirror with high transmission at the LD pump wavelength, high reflectivity at the LDPSSL wavelength; M2, reflector at the LDPSSL wavelength; SSL, solid state laser; L1, spherical lens; L2, cylindrical lens; M3, mirror deposited directly onto the fibre surface; FL, fibre laser. (*a*) Shows a simple longitudinal geometry; (*b*) shows a remotely sited LD coupled to the SSL through an optical fibre; (*c*) is a transversely pumped solid state laser; and (*d*) shows an LD-pumped waveguide laser, in this case a fibre laser.

effects which are masked in other lasers may be exploited in the LDPSSL.

(7) A wide variety of LDPSSL configurations have been adopted. Some of the common schemes are illustrated in figure 1. The LD may be coupled directly to the laser material (figure 1(*a*)) or remotely via an optical fibre, (figure 1(*b*)). The device may be longitudinally pumped, (figure 1(*a*), (*b*)), or transversely pumped, (figure 1(*c*)). The laser host may be bulk or in the form of a waveguide or optical fibre, (figure 1(*d*)).

Most of the advantages of the LDPSSL arise from features of the LD and the solid state laser component simply overcomes some of the disadvantages of the LD. When looking further into the future some of the disadvantages of LDs may be removed. For example, the beam quality and output power of LDs are likely to improve. However, it is unlikely that the peak power capabilities and energy storage capacity of the solid state laser will be superseded by the LD.

The LDPSSL field has expanded enormously over the past five years and now covers bulk lasers, fibre lasers and crystal waveguide lasers as well as the division between continuous wave lasers and pulsed lasers. In general, this review is restricted to continuous wave bulk lasers although brief mention will be made of the various waveguide lasers and pulsed operation.

2. Overview of laser diode pumped solid state lasers

An important point worth emphasizing is that LDPSSLs are not a new concept. Indeed the first publications which used a semiconductor pn junction either as a light emitting diode (LED) or as a LD to optically pump a laser date from the 1960s [3–5]. Due to the poor performance of these early pump sources, where CW operation was difficult even at cryogenic temperatures, relatively little attention was paid to LDPSSLs.

The story really became interesting when reliable LDs became available in the early 1980s. These LDs could be operated either in CW or pulsed mode at room temperature and had long lifetimes in the region of 100s to 1000s of hours. Moreover the LDs were available at interesting wavelengths around 807 nm which corresponds to a strong absorption line in Nd:YAG. Commercially, the main driving force behind the development of the LDs was usage in mass markets, such as the compact disc player which required sources around 780 nm. Additional applications requiring higher powered devices are laser printers and optical memories. The use of LDs to pump solid state lasers was recognized, with the main applications seen to arise from tasks which require efficient, reliable, long-lived optical sources. These tasks could be remote sensing from satellites, space-based communications and wind shear sensing from aircraft or at airports. Clearly a satellite-based system cannot be routinely serviced and must be efficient.

Reliable LDs with continuous wave powers of 100 mW and the correct wavelength range (790–810 nm) for pumping solid state laser materials stimulated scientific and commercial interest in LDPSSLs. The increasing activity resulting from the availability and affordability of LDs is reflected by the dramatic increase in the publication rate of scientific papers which mention LDPSSL in the title or abstract. Since the late sixties the publication rate remained constant at the few (0 to 4) papers a year level arising mainly from laboratories with special access to LDs or theoretically interested in the commercial or scientific possibilities presented by these lasers. Since 1986 the publication rate has increase fortyfold to more than 150 papers published in 1990. Over the same period the continuous power output available from commercial LDs increased to 15 W while the cost per Watt decreased as the demand for LDs increased. The LDPSSL can now be puchased as a complete unit from a variety of vendors and produces output in a range of sophisticated formats, for example

single-frequency sources, frequency-doubled sources or modelocked sources. It is fair to say that the main barrier to extensive exploitation of LDPSSLs is still the high cost of LDs in comparison with the mature technologies associated with flashlamp-pumped systems. The technical problems encountered when using LDs as pump sources are being solved but attention is still being paid to coping with the thermal sensitivity of LDs and designing efficient ways of coupling light from the LD into the solid state laser material.

2.1. Early laser diode pumped solid state lasers

Much of the early work on LDPSSLs has been reviewed up to the end of 1987 in an article by Fan and Byer [6]. A brief summary of the salient points will be given here. The earliest example of a LDPSSL was $U^{3+}:CaF_2$ which lases at 2.613 μm and was pumped at 840 nm [7]. Subsequent interest has concentrated predominantly on rare earth (RE) ions doped into various hosts. The ubiquitous example is of course Nd:YAG which was first LD pumped by Ross in 1968 [4], although another RE ion, Dy^{2+}, had earlier been pumped by an array of light emitting diodes [8]. Nd:YAG and other Nd-doped laser hosts including Nd:glass and Nd:YLF have had a long history as solid state laser materials since Nd laser operation was first demonstrated in 1961 [9]. Yttrium aluminium garnet (YAG) was demonstrated as a host in 1964 [10] and since then has become one of the most widely used solid state laser materials.

The early work on LDPSSLs used a traverse pumping geometry (see section 4.1) which is convenient when using a number of sources with poor beam quality. Longitudinally or end-pumped LDPSSLs (see section 4.2) were first demonstrated in 1973 [11–14]. The advantages of this latter approach in minimizing the laser threshold was noted, as was the disadvantage of limited power scaling due to the problem of coupling the output of many LD sources into the gain medium.

Fibre optic waveguides have also been doped with various RE ions and pumped by semiconductor lasers. Fibre lasers [15, 16] were realized shortly after the discovery of the laser and were initially transversely pumped by the crude but effective technique of coiling a fibre round a flashlamp. Mirrors were butted up to the end of the fibre or directly deposited onto the fibre ends. The motivation for using the fibre geometry for end pumping by LDs was the long interaction length that could be achieved between the pump beam and the gain medium without diffraction effects reducing the pump intensity. In this way low threshold could be reached [17–20]. The development of techniques to dope single transverse mode optical fibres with RE ions [21], in such a way that low propagation losses occurred, allowed the construction of single mode fibre lasers [22]. These devices proved to be easily LD pumpable provided that efficient coupling between the LD and the fibre could be achieved [23]. Moreover, the long interaction lengths allows the use of RE ions or pump absorptions where very long absorption lengths made bulk lasers impractical. Probably the most important commercial application of this technology is the development of the erbium-doped fibre amplifier which amplifies near 1.54 μm [24]. This corresponds to the low loss window in silica fibre and is used for long distance communications. This device is LD pumpable at 980 nm and 1.48 μm.

LDPSSLs have also been used to generate various type of output. Q-switching and mode locking have been used to increase the peak power from these sources while single longitudinal mode operation demonstrates their good spectral properties. Further discussion of these topics will be given in sections 6 and 7.

3. Laser diodes

This section describes the main attributes of LDs commonly used to pump solid state lasers. The features of LDs that are important in the design and operation of LDPSSLs are presented. Full details of the constructional techniques of LDs may be found in a review by Streifer *et al* [2]. LD technology is rapidly changing as evidenced by the change in CW powers available from commercial LDs mentioned previously, consequently the data presented in this section may become rapidly out of date.

The wavelength and lifetime properties of LDs will be discussed followed by the optical properties of LDs. The types of problem found when coupling the output of LDs, LD arrays and LD bars into solid state laser materials will also be discussed.

3.1. Wavelength

The wavelength at which LDs operate is dictated by the size of the band gap, since the light arises from the recombination of electrons and holes in a pn junction. The band gap may be tuned in size by two main processes:

(i) altering the composition of the host material,
(ii) changing the temperature of the host material.

These properties will be discussed in turn. Other physical effects such as the application of pressure may also change the bandgap but they tend to produce too small an effect to be useful.

3.1.1. Material. Selecting the composition of the host material enables LDs to be constructed with wavelengths between 600 nm and approximately 30 μm in the infrared. Over much of this region the output power and lifetime of LDs is remarkably poor. Only in wavelength regions where strong commercial or military interest is present have sufficient resources been deployed to develop an efficient and long-lived device. Notable examples of this process have occurred at 1.5 μm and 1.3 μm, which are important telecommunications wavelengths, and near 800 nm which is important for communications, entertainment and medical applications. Only in the vicinity of 800 nm

have high-powered devices been built. The driving force has been military applications including pumping Nd-doped solid state lasers. It is interesting to note that strained layer InGaAs devices with wavelengths in the range 870 nm–1.1 μm region are being actively developed for use with erbium-doped fibre amplifier for use in 1.5 μm long-haul communication systems. Both single stripe and array devices are built, so high power may be available in this region shortly.

The 800 nm LDs are based on $Ga_{1-x}Al_xAs$ material where $x \approx 0.09$ for devices emitting near 807 nm which is the Nd:YAG absorption line. Varying the amount of aluminium changes the emission wavelength over the range 680–900 nm with decreasing efficiency and lifetime at either end of the range. Strict control on the quantity of Al doping is essential since varying the doping level by ≈1% leads to wavelength shifts of the order of 1 nm.

3.1.2. Temperature. Fine tuning the temperature of the LD causes a change in wavelength. For GaAlAs devices the wavelength tunes at an approximate rate of $+0.25\ nm\ °C^{-1}$ mainly due to the change in band gap with temperature. This feature is used to tune the LD into coincidence with the absorption bands of RE ions. Normally the lasers will be cooled down, since this gives a longer lifetime for the LD. It is usual to specify the room-temperature wavelength of the LD some 5 nm longer than the RE absorption feature that will be pumped. Simple Peltier coolers can provide a temperature change of about 40 °C corresponding to a wavelength shift of 10 nm. The Nd:YAG absorption linewidth is ≈2 nm so the diode temperature has to be set to better than ±4 °C, which is not too demanding in the laboratory. The influence of temperature on the wavelength of the LD causes problems of packaging an LDPSSL. An ambient temperature range of, say, −20 to +50 °C would require a substantial investment in temperature control that would reduce the system efficiency and increase the weight and size of the final device.

Pulsed LDs suffer from a transient thermal wavelength shift. Since the current is pulsed through the LD, the temperature is never in equilibrium and a transient wavelength shift occurs. The wavelength increases during the optical pulse. Measurements of this effect have revealed shifts of ≈5 nm. Shifts of this magnitude are larger than the absorption linewidth of many solid state laser materials [2, 25]. Account has to be taken of this effect when predicting the efficiency of pulsed LDPSSLs.

3.1.3. Lifetime. Commercial LDs can have room-temperature lifetimes, defined as the mean time to failure, of 3×10^4 h for CW devices and around 10^9 pulses for pulsed LDs. These values should be compared with lifetimes for arc lamps, for CW pumping, of 200 h and flashlamps, for pulsed pumping, of 10^7 shots. Failure of the LD may be sudden and catastrophic or gradual, leading to an increase in current required to maintain a specific output power.

There are three main causes of LD failure:

(i) degradation of the laser mirrors or facets leading to a lower reflectivity or higher absorption losses;

(ii) increasing resistance of the electrical contacts to the laser causing resistive losses and heating;

(iii) internal damage arising from lattice defects occurring within, or migrating to, the active region of the laser, giving rise to higher optical absorption.

The long lifetimes mean that it is usually impractical to measure the lifetimes directly under normal operating conditions. The usual procedure is to use accelerated testing at raised temperatures. Three failure modes may be identified during these tests:

(1) a group of failures occurs during initial operation or 'burn in', which is attributable to dark line defects;

(2) gradual degradation of the LD and an increase in current required to maintain a specific output power is observed at all temperatures;

(3) above about 30 °C sudden failures occur which are due to an increase in resistance of the contacts.

There are two further causes of LD mortality which arise from the way in which they are used. LDs are particularly prone to optical damage to the laser facets. Damage, which is normally localized melting, occurs either because a current spike drives the device beyond its rated electrical or optical limits or because an inadvertent retroreflection raises the local intensity beyond its rated level. The current supplied to an LD should be properly regulated and filtered to remove mains noise and switching transients and anti-static precautions should be taken when handling the LD. Appropriate care is required when aligning coupling optics to avoid retroreflections. The feedback can cause an increase in the apparent reflectivity of the LD facets leading to a larger circulating optical field within the LD cavity. The unpumped regions of the semiconductor adjacent to the facet see a higher level of heating due to increased absorption which can eventually lead to local melting of the facet and termination of the laser action. This is called catastrophic optical damage for obvious reasons and its implications for the design of LDs is considered in the next section.

3.2. Optical properties of laser diodes

LDs can be fabricated in a number of different geometries. The main limit to high-power LDs commonly used to pump solid state lasers is melting of the facets due to absorption of the laser light in unpumped regions of the active layer. This is catastrophic optical damage and occurs at intensities of a few $MW\ cm^{-2}$. Typical dimensions of the emission region of a double-heterostructure quantum well laser might be 3×1 μm indicating a maximum power of the order of 30 mW. Increased output power can be achieved most simply by increasing the width of the strip leading to the so called broadstripe array. The problem with this

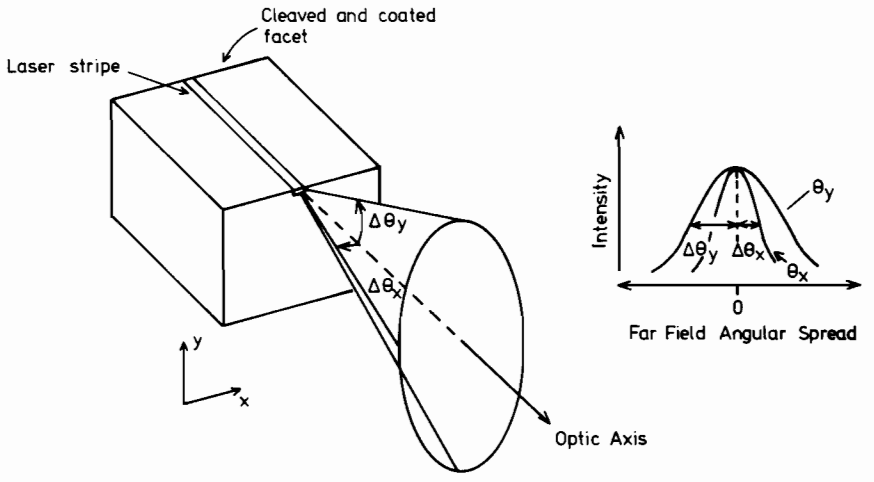

Figure 2. The elliptic beam shape arising from the transverse dimensions of a single LD stripe. The stripe dimension is typically 3 μm in the *X* plane and 1 μm in the *Y* plane which is the origin of the greater divergence in the *Y* plane.

approach is that the LD output is no longer constrained to be in a single transverse mode and it is found that the LD lifetime is compromised due to filamentary operation which can cause optical damage. This problem can be avoided by making an array of LD stripes each perhaps $3 \times 1\,\mu$m on 10 μm centres. Normally, for LD pumping of solid state lasers the stripes forming the arrays will be partially coherent through a small amount of evanescent coupling between adjacent stripes. Large coupling between the stripes, while enforcing coherent output, also places an upper limit on the number of stripes forming the array to prevent transverse lasing and other parasitic effects which limit the output power. CW devices might consist of 10, 20 or 50 stripes with overall apertures of 100 μm, 200 μm or 500 μm respectively. The total output power will range from 500 mW for the narrower device to 3 W for the largest device which ensures that the output per stripe is about 50 mW ensuring a low risk of optical damage and a reasonable lifetime.

3.2.1. Single stripe devices. The best transverse mode quality is obtained from single stripe devices. The low ellipticity of a source with dimensions of $3 \times 1\,\mu$m ensures that the output power may be efficiently coupled into optical fibre or into solid state laser materials. Single LDs may provide up to 150 mW in a single transverse mode. The shape of the output beam from a single strip device is shown in figure 2.

The elliptical output from these devices may be circularized using a relatively simple optical arrangement as shown in figure 3. A simplified analysis of this configuration involving a spherical condensing lens of focal length f and a prism beam expander (PBE) with expansion M in the plane parallel to the long dimension of the LD (the x plane) is presented here. The lens is placed d_1 from the LD and PBE is d_2 from the lens. The diode output will be treated as an elliptical Gaussian beam with waists in the same plane, $z = 0$, and confocal parameters

$$q_x = \frac{-i\lambda}{\pi\omega_x^2}$$

$$q_y = \frac{-i\lambda}{\pi\omega_y^2}$$

in the x and y plane respectively. The prism beam expander (PBE) operates in the y plane and will be represented for the purposes of this analysis by the ABCD matrix:

$$\begin{bmatrix} M & D + \dfrac{l}{n} + \dfrac{l}{Mn} \\ 0 & 1/M \end{bmatrix}$$

where M is the magnification [26–32]. The separation of the prisms is D while the path length within the prisms of refractive index n is l. Assuming that the lens is positioned so that $d_1 \approx f$ and the lens PBE spacing is neglected ($d_2 = 0$), then the net ABCD matrix for a translation from the LD to after the PBE may be calculated to be:

$$\begin{bmatrix} 1 & d_1 \\ -1/f & 1 - d_1/f \end{bmatrix} \qquad \begin{bmatrix} M & Md_1 \\ -\dfrac{1}{fM} & \dfrac{1}{M}(1 - d_1/f) \end{bmatrix}$$

in the y and x plane respectively. The additional assumption that the PBE is ideal

$$\left(D + \frac{l}{n} + \frac{l}{Mn} \approx 0\right)$$

has been used.

If the optical system is to circularize the beam, then after the PBE, both planes must have identical complex beam parameter q. Using the ABCD rule to calculate

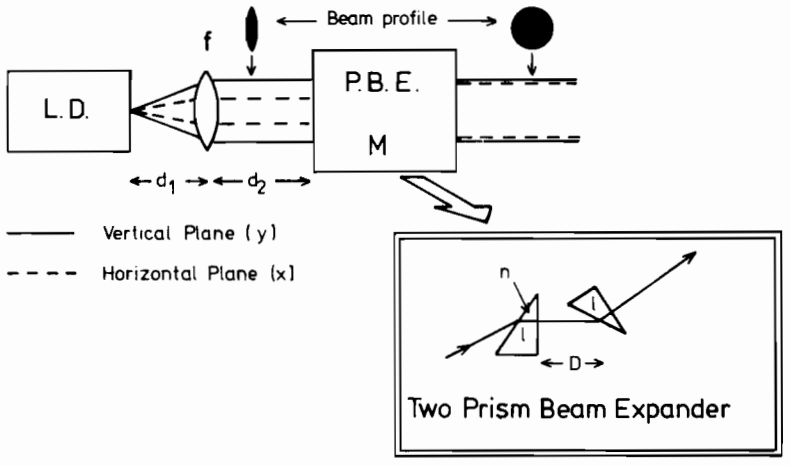

Figure 3. Simple optical scheme commonly adopted to circularize the output of an LD.

the complex beam parameter after the optical system yields:

$$q = \frac{q_y + d_1}{-(1/f)q_y + (1 - d_1/f)} = \frac{Mq_x + Md_1}{-(1/Mf)q_x + (1/M)(1 - d_1/f)}.$$

The equality holds provided that $q_x = M^2 q_y$ where $|q_x|$, $|q_y| \ll d$. The latter inequality holds very well since $w_x = 5\,\mu$m, $\lambda = 800$ nm and $|q_{x,y}| = 10^{-4}$ m, $d_1 = 10^{-2}$ m. In order for the beam to be circularized after the PBE, the size of the emission regions in the x and y planes have to be related by $\omega_y = \omega_x/M$. Typical values of M are in the range $M = 3$–7.

The coupling optics can have very high transmissions of 95% to 99% since the spherical lens and the PBE may be anti-reflection coated. Additional components such as cylindrical lenses may be included to improve the performance of the anamorphic optical system and can lead to equal spot sizes in the x and y planes [32].

3.2.2. Laser diode arrays. Frequently, LDPSSLs are pumped by LD arrays in order to achieve high output powers. As has been noted, the simplest way to increase the output power from a single LD is to increase the width of the emitting region either by fabricating a number of LD stripes in close proximity so that there is a series of emitting regions, or by enlarging the width of the electrically pumped region.

The output of arrays lies in the region of 200 mW to 3 W CW output at present. True arrays of LD stripes tend to be partially coherent and may exhibit the two-lobe structure in the far field characteristic of a pi phase changes due to evanescent coupling between adjacent stripes. This feature appears less obvious as the output power and number of stripes increase due to reduced coherence across the array. The broad stripe arrays are multi-transverse mode devices and the beam quality depends on how hard they are driven.

Both types of array are used to pump solid state lasers longitudinally. The emitting region may be overall 500 μm wide by 1 μm deep, so the divergence is different in the two planes. The direct coupling scheme, illustrated in figure 1(*a*) and described in section 3.2.1, is often used to couple light into the solid state laser material.

3.2.3. Laser diode bars. The length of arrays is limited by thermal problems related to removing the heat generated in the active region. Initially this is conducted through the LD substrate material. The scaling of CW arrays to higher power levels (5 W, 10 W and 15 W devices) has been achieved using a bar structure. The 5 W and 10 W (15 W) devices are composed of twelve (thirty-five) individual arrays with an aperture of 200 μm (100 μm) which are grown on a single 1 cm substrate whose length is limited by growth constraints. The complete bar, as this device is called, is then used as a unit with all the arrays being electrically connected in parallel. The output of these devices is predominantly incoherent since there is no possibility of coupling between adjacent arrays. It is also a difficult device to work with and to couple into solid state laser materials particularly in longitudinal geometries. LD bars are normally used in pulsed mode in side-pumped geometries where the high peak powers achievable overcome the low gain inherent in this scheme [33, 34].

Since bars are made up of a number of independent sources, the wavelength distribution has to be very carefully controlled during the manufacturing stage in order that efficient pumping of solid state lasers is possible. The wavelength change along a bar might be 2–3 nm due to small material variations.

3.3. Alternative optical delivery schemes

The optical coupling schemes that have been discussed so far rely on circularizing the output from an LD array or bar using bulk optics. An intriguing development is to use the solid state laser material in close proximity

to the LD with no intervening optics. This process is capable of allowing the construction and packaging of a device which is not much larger than the LD device itself. Under these conditions the output of the LDPSSL can be in an excellent TEM_{00} mode with the added bonus of single longitudinal mode operation in many cases. Good beam quality arises through the transverse mode selection of the pumped region which, in the short absorption length, does not become larger than the lasing mode. Additional processes such as thermal lensing may help the stability of these cavities. Single longitudinal mode operation is enforced by ensuring that the length of the laser is sufficiently short that only a single longitudinal mode of the laser cavity lies under the gain curve [35, 36]. This requirement also aids the formation of a good single spatial mode. The short lengths that are required for single-frequency operation (typically 750 μm for Nd:YAG) means that the absorption of the pump light is small, resulting in a reduced overall system efficiency.

Many LD arrays can now be purchased with an optical fibre pigtail [37]. A multimode optical fibre with a typical core diameter of 100–200 μm is placed close to the LD facet and collects about 50% of the emitted light. The fibre provides simple handling and remote siting of the LD output so that the LDPSSL can be decoupled from the LD as shown in figure 1(*b*). LD bars can also be coupled in this fashion using a single fibre for each emitting region along the bar. The fibres can then be bundled to produce a high average power of up to 10 W from a 380 μm aperture. In this case, of course, the output from each region (and fibre) is incoherent.

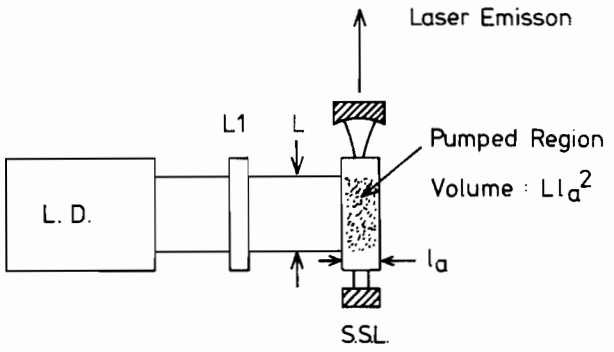

Figure 4. A schematic diagram of a transverse pumped LDPSSL. The notation is: LD, laser diode; L1, cylindrical lens; L, the length of the line focus in the SSL; SSL, solid state laser; l_a, absorption length of the pump wavelength.

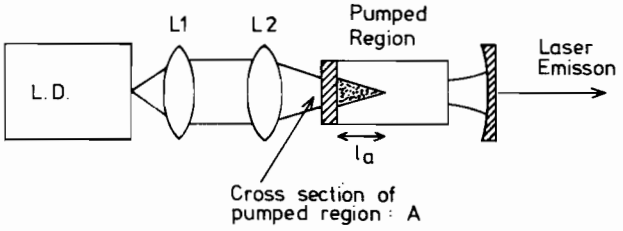

Figure 5. A schematic longitudinal pumping geometry. The notation is: LD, laser diode; L1, L2, collimating and focusing lens respectively; l_a, absorption length of the pumped region.

4. Pumping schemes

Most pumping schemes may be categorized as either longitudinally pumped or transversely pumped. The choice of pumping scheme depends primarily on the beam quality of the pump source and the power available from that source. Low-quality beams available from LEDs and early LDs were difficult to focus to small spot sizes, so the pumping geometry tended to be the transverse scheme discussed in section 4.1. The large surface area of the laser host was illuminated in a direction perpendicular to the laser emission as shown in figure 1(*c*) and figure 4. Transverse pumping allows scaling to high-power operation by the simple mechanism of increasing the number of pump sources placed around the laser rod. The advent of LDs with better quality beams allowed the use of longitudinally pumped lasers, shown in figure 1(*a*, *b*) and figure 5, and discussed in section 4.2, which have the advantage of low thresholds due to the small pumped area.

Transverse and longitudinal pumping geometries are not unique to LDPSSLs. All optically pumped lasers use one or the other system. Continuous wave dye lasers or Ti:sapphire lasers tend to be longitudinally pumped by Ar^+ or Kr^+ ion lasers since these provide the lowest threshold, whereas dye lasers and amplifiers pumped by excimer or nitrogen lasers are usually transversely pumped due to the poor beam quality from these lasers [38–40].

4.1. Transverse pumping scheme

The primary consideration for any pumping scheme is that the incident light must be efficiently absorbed within the laser host. For transverse pumping shown in figure 4 this implies that the thickness of the laser material should be sufficient to absorb a significant fraction of the pump light. However, the material cannot be too thick otherwise a portion will remain unpumped. The simplest approach, which suffices for this discussion and which neglects refinements such as retroreflectors for multipassing the pump light or multiple pump sources, is to assume that the laser material is one absorption length l_a thick:

$$l_a = 1/N\sigma_a$$

where σ_a is the absorption cross section for the pump light and N is the number density of the active ions. Assuming that there is a monochromatic continuous wave power P incident on the laser material over a length L the steady state population inversion n, in the absence of stimulated emission, is

$$n = \frac{P}{h\nu}\frac{\tau}{l_a^2 L}$$

where τ is the fluorescence lifetime of the upper laser

level and ν is the pump frequency. The steady state gain may be estimated to be

$$G = \exp(n\sigma_e L) = \exp\frac{P}{h\nu}\frac{\tau\sigma_e}{l_a^2}$$

where σ_e is the stimulated emission cross section at the laser wavelength. The important point to notice is that the gain is strongly dependent on the absorption length l_a and not on the length of the laser material. For Nd:YAG at 807 nm the absorption length is about 2 mm leading to the requirement for relatively high pump powers. In most solid state laser materials the absorption length is relatively long and cannot easily be decreased by increasing the dopant level, due to problems associated with the interaction of the ions at high concentrations. In Nd:YAG the fluorescence lifetime reduces due to non-radiative de-excitation caused by other ions. Other RE ions exhibit clustering at high concentrations, which allows significant interactions, such as energy transfer, to take place which reduce the efficiency of the pumping process. The only parameter which is at the disposal of the laser designer is the pump power P which cannot always be arbitrarily varied. Since pulsed LDs produce high peak powers which are easily coupled into large volumes, most transversely pumped LDPSSLs are pulsed.

4.2. Longitudinal pumping

A somewhat more sophisticated approach which allows lower laser thresholds is to longitudinally pump the laser material as shown in figure 5. The optical pump beam is directed longitudinally along the laser axis. It is focused to a spot size of area A which will be assumed constant throughout a length L of the laser material. In a similar fashion to the previous section the gain may be estimated to be

$$G = \exp\frac{P}{h\nu}\frac{\tau\sigma_e}{A}.$$

The gain has no dependence on the absorption length of the material provided that $l_a < L$ which is consistent with the earlier assumption that the pump power is substantially absorbed within the laser material.

If the beam quality of the pump laser is good enough the area can be quite small (perhaps 100 μm^2) and the gain G may be quite large. LDs with good beam quality tend to be relatively low-power devices as was observed in section 3, nevertheless the increased gain due to the tight focusing more than compensates for the low power and enables the construction of efficient lasers.

It would appear that the gain may be made arbitrarily large by reducing the cross sectional area of the pump beam. Due to the increased diffraction spread of the pump beam the assumption made in the analysis that the area of the pump beam was constant throughout the sample would be violated. By manipulating the structure of the material the diffracting effects of light may be avoided by producing an optical light guide by varying the refractive index transversely. These are commonly in the form of single transverse mode optical fibres, but planar and stripe waveguides in bulk crystalline materials have been demonstrated, and enable beams with transverse dimensions of the order of the wavelength of light to be maintained over a distance of kilometres. Optical fibres may be doped with many different RE ions and have been used to make lasers which can exhibit extremely low thresholds.

An additional advantage of longitudinal pumping over transverse pumping is that the size of the pumped region may be easily matched to the transverse dimensions of the laser mode, thus forcing single transverse mode operation without the need to use lossy mode selecting apertures. In addition, the good overlap of the pump and laser mode ensures good extraction efficiency [39, 41]. Longitudinal pumping, however, does suffer from the disadvantage that high-power operation is difficult due to the problems of physically coupling many LDs into the small pumped volume. The use of remote fibre coupled LDs or spatially stacking the output of LDs may overcome this to an extent [42, 43].

5. Specific examples of LDPSSLs

In this section we consider the performance of a range of specific LDPSSLs. Where appropriate, both CW and pulsed operation will be discussed, although the use of modelocking techniques to produce ultrashort pulses will be considered in detail in section 6. We begin by considering in some detail the LD-pumped Nd:YAG laser, which is certainly the best studied LD-pumped system. We will then consider the performance of the LD-pumped Nd:X laser, where X is any one of a number of host materials, and also LD-pumped stoichiometric materials. Other RE-doped lasers will then be discussed, and we will also consider the recent interest in the pumping of tunable chromium-doped lasers with visible LDs. Finally, optical fibre lasers and crystal waveguide lasers will be briefly discussed. This section is by no mean exhaustive, but rather is intended to give the reader a good idea of the current state of research in the field of LDPSSLs. It thus necessarily concentrates on relatively recent work. For a more historical overview of the performance of various LDPSSLs the reader is referred to the review article of Fan and Byer [6].

5.1. Nd-doped laser diode pumped lasers

The trivalent neodymium ion was the first of the RE ions to be used in a laser, and it is the dopant which has received most attention in the field of LDPSSLs. The Nd^{3+} ion has a strong absorption at 807 nm, which coincides with the emission wavelength of commercially available GaAs and GaAlAs LDs. Most of the research reported on LD-pumped Nd-doped lasers

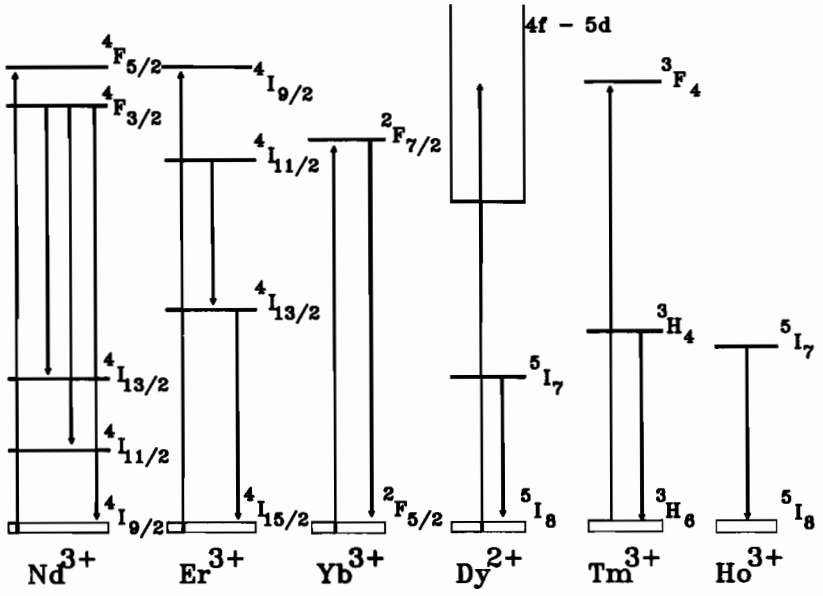

Figure 6. Simplified energy level diagrams for some of the most important RE ions. The approximate absorption wavelengths are: Nd^{3+}: $^4I_{9/2}$–$^4F_{5/2}$: 807 nm; Er^{3+}: $^4I_{15/2}$–$^4I_{9/2}$: 797 nm; Yb^{3+}: $^2F_{5/2}$–$^2F_{7/2}$: 950 nm; Dy^{2+}: $^5I_8$–(4f–5d): ~720 nm; Tm^{3+}: $^3H_6$–$^3F_4$: 780 nm; Ho^{3+}: see text and figure 8. The approximate emission wavelengths are: Dy^{2+} 2.4 μm; for other materials, refer to the relevant sections in the text.

has concentrated on the four-level high-gain $^4F_{3/2}$–$^4I_{11/2}$ transition, which corresponds to a laser output in the region of 1.06 μm. However, work has also been reported on the 1.3 μm $^4F_{3/2}$–$^4I_{13/2}$ transition, and on the three-level 946 nm $^4F_{3/2}$–$^4I_{9/2}$ transition. In this paper, all Nd-doped laser results refer to the 1.06 μm transition unless otherwise stated. Figure 6 shows a simplified energy level diagram for Nd and several other important RE ions.

The question of whether one host medium is any 'better' than another is not a trivial one, and depends to some extent on the application for which the laser is intended. The choice of host medium affects the upper state lifetime of the Nd ion, as well as its absorption and emission spectra. A broad absorption spectrum is useful for LD pumping, since it decreases the necessity for precise temperature control of the LD wavelength. This is particularly useful for pumping with pulsed LDs where the wavelength of the LD can vary considerably during the current pulse [2, 25]. A broader emission spectrum, while increasing the pumping threshold, offers the possibility of obtaining shorter pulses via modelocking techniques. It also leads to a reduced stimulated emission cross section, which allows for a larger amount of energy to be stored in the upper laser level. This is particularly important for Q-switched operation.

The upper state lifetime is another important parameter for energy storage which can vary significantly with the choice of host medium. One problem which affects Nd^{3+}-doped laser materials is that of concentration quenching of the upper state lifetime, where the lifetime decreases with increasing Nd^{3+} concentration. This leads to an increase in pump threshold. However, high doping is often desirable in LDPSSLs so that the pump radiation can be absorbed in a smaller volume, yielding a lower pump power threshold. One class of material in which this problem may be overcome is that of stoichiometric materials, where the Nd^{3+} is a constituent component of the material, rather than a dopant. These materials can have a much higher (greater than an order of magnitude) Nd^{3+} concentration than, for example, Nd:YAG, yielding a very high absorption of pump radiation in a small volume. These materials will be considered later in this section.

5.1.1. The LD-pumped Nd:YAG laser. The Nd:YAG (yttrium aluminium garnet) laser has become the most common LDPSSL for a variety of reasons. The advantages of the Nd^{3+} ion as a dopant have been mentioned previously. The cubic structure of YAG favours a narrow emission spectrum, which leads to a low threshold for laser operation. However, the level of neodymium doping in YAG is limited to about 1.5% due to concentration quenching of the upper state lifetime. Some of the relevant optical parameters for Nd-doped lasers are shown in table 1 and will be referred to throughout this section. The YAG host is noted for its hardness, high thermal conductivity and good optical quality. This section has been divided into several subsections due to the large volume of work which has been published on the LD pumped Nd:YAG laser.

5.1.1.1. Longitudinally pumped Nd:YAG rod lasers. The highest overall efficiencies are generally obtained from the longitudinally, or end-pumped geometry, due to the excellent matching that can be obtained between

Table 1. The various material parameters that are obtained from Nd doped into some common laser hosts†.

	λ_L	σ	τ	λ_P	$\Delta\lambda_P$	$\Delta\lambda_e$
Nd:YAG	1.064	6.5	230	807.5	1.2	0.5
Nd:YLF			480			1.4
σ	1.053	3.2		806.0	2.8	
π	1.047			792.5	1.7	
Nd:BEL [84, 86]			150		6.9	3.4
X	1.070	1.2		811.0		
Y	1.079	0.7		811.0		
Z	1.079	0.4		810.5		
Nd:YAP [90]	1.079		150	800.0		
Nd:GSGG [93, 95]	1.061	1.31	284	808.0		1.2
Nd:YVO_4 [87]	1.06	20.1	98	809	20	1
Nd:$CaYAlO_4$ [96]	1.081	8.9	113	805	5	11
Nd:glass (LG760 phosphate glass)	1.053	4.2	350	801	14	20

† In this table, the following symbols and units are used: λ_L, lasing wavelength for the $^4F_{3/2}$–$^4I_{11/2}$ transition (μm); σ, stimulated emission cross section ($\times 10^{-19}$ cm^2); τ, upper level lifetime (μs); λ_P, peak of absorption spectrum in the 800 nm region (nm); $\Delta\lambda_P$, FWHM of absorption spectrum in the 800 nm region (nm); $\Delta\lambda_e$, FWHM of fluorescent spectrum (nm). The numbers in brackets in the materials column refer to the references (and references therein) from which most of the data were obtained.

the focused pump beam and the SSL TEM_{00} mode. The first highly efficient LD end-pumped Nd:YAG laser was reported by Sipes [44], who obtained an output of 80 mW at an overall (electrical-to-optical) efficiency of 8%. At the time this was the highest overall CW efficiency reported for an Nd:YAG laser. Berger *et al* [45] reported an overall efficiency of 10.8% and an output power of 415 mW from an Nd:YAG laser end-pumped by an LD array (LDA). The output power available from this system was limited by the power from the pump source. Simply increasing the width of the array to increase its power would reduce the ability of the collecting and focusing optics to match the highly asymmetric pump beam to the Nd:YAG TEM_{00} mode. Berger *et al* [43] reported a means of overcoming this problem by coupling the output from seven LDAs into a fibre bundle, and focusing the output from the bundle onto the Nd:YAG rod. An output power of 660 mW was obtained, although at a reduced overall efficiency of 4.4%. The reduction in efficiency was mainly due to the coupling of the pump light into the fibre. Fan *et al* [42] proposed another method for scaling end-pumped lasers to higher powers, whereby a number of LDs are placed close together, and each is collimated individually. Using three LDAs, this technique yielded an output power of greater than 500 mW with an optical slope efficiency of 58%. More recently, Shannon and Wallace [46] end-pumped an Nd:YAG laser using a 10 W LD bar. To match the focused pump beam to the laser TEM_{00} mode, a cavity was designed which had an elliptical TEM_{00} mode. An output power of 1.9 W was obtained, which represented an optical-to-optical efficiency of 19%. Tidwell *et al* [47] used a geometric multiplexing scheme in which the output from four 10 W LD bars was used to end pump an Nd:YAG rod. 15 W of multimode output power was obtained, which corresponded to an overall efficiency of 10.5%. The maximum TEM_{00} output power was 3 W. Yamaguchi and Imai [48] used 20 gradient index (GRIN) lenses to collimate the 20 stripes of an LDA. Using this technique, 1.33 W of output was obtained from an Nd:YAG laser with 4.58 W of pump power.

Several authors have reported LD-pumped laser operation of the 946 nm $^4F_{3/2}$–$^4I_{9/2}$ transition in Nd:YAG [49–53]. Risk and Lenth [50] reported on the room-temperature operation of this laser, and obtained 42 mW of TEM_{00} output. This was achieved for a very low (0.7%) output coupling, which the authors noted was not optimum. 946 nm Nd:YAG laser operation has recently been reported [51, 52] using laser cavities which resonate both the pump radiation and the 946 nm laser radiation. Kozlovsky and Risk [51] obtained 25 mW output power for 51.8 mW pump power incident on the crystal.

5.1.1.2. Transversely pumped Nd:YAG rod and slab lasers. The limitations imposed on efficient coupling using end pumping mean that to obtain higher powers it is necessary to use a scheme whereby a laser rod or slab is pumped using a transverse pumping geometry. A disadvantage of the transverse-pumped geometry is that the efficiencies for TEM_{00} operation generally tend to be much lower than for the end-pumped case due to poor mode matching. Several authors [34, 54–56] have published results for pulsed systems. Optical slope efficiencies of 23% for slabs [54] and 54% for rods [56] have been obtained. The high efficiency obtained by Hays *et al* [56] was for multimode operation. Berger *et al* [57] reported a novel scheme combining low-power CW LD end pumping and high-power pulsed LD transverse pumping. This scheme was found to suppress

relaxation oscillations, increase pulse energy, and prevented the laser operating in higher order transverse modes.

Transversely pumped CW Nd:YAG lasers have also been reported [58, 59]. Burnham and Hays [59] used four CW LDAs to pump a Nd:YAG rod transversely. 3.3 W of multimode output were obtained, at an overall efficiency of 3.5%. As expected, the efficiency of TEM_{00} operation was lower, at 2%.

5.1.1.3. Longitudinally pumped Nd:YAG slab lasers. Higher TEM_{00} CW powers than those obtained using longitudinal pumping of rods or transverse pumping of rods and slabs have been obtained by the longitudinal pumping of Nd:YAG slab lasers [60, 61]. Baer *et al* [60] reported a TEM_{00} output power of 3.8 W (the optical slope efficiency was 46%) using a tightly folded resonator. This was designed to provide a laser mode to match the collimated output from a 10 W LD bar. Watanabe *et al* [61] described the use of twenty 1 W LDAs, each focused into a fibre before being directed onto appropriate points on an Nd:YAG slab. They obtained 3.5 W of TEM_{00} output, at an optical slope efficiency of 37%. As in the work of Berger *et al* [43], however, the overall efficiency was significantly reduced due to the use of fibres. Another technique still [62], where the output from four 500 mW LDs was used to pump each reflection point in an Nd:YAG slab laser, has yielded 685 mW of TEM_{00} output power at an overall efficiency of 8.5%. The authors note that this system should be readily scalable to higher powers.

5.1.1.4. The Q-switched LD pumped Nd:YAG laser. The long upper state lifetimes (100 s of μs or longer) of solid state laser transitions mean that large amounts of energy can be stored in the upper laser level. This means that LDPSSLs are good candidates for high peak power Q-switched operation. There has been much work reported on the Q-switched operation of the LD pumped Nd:YAG laser [46, 63–68]. Gerstenberger *et al* [66] used high peak power (120 W) pulsed LD bars as a transverse pump source, and obtained 587 kW of peak power in a 7.5 ns output pulse. For longitudinal-pumped operation, Grossman *et al* [68] obtained peak powers of 1.1 kW at 1.3 μm (pulse width 22 ns) and 7 kW at 1.06 μm (pulse width 6 ns). Each of these results was obtained using active Q-switching. Morris and Pollock [67] obtained a peak power of greater than 1 kW in pulses of duration 20–30 ns using passive Q-switching where F_2^- colour centres in lithium fluoride were used as a saturable absorber. These colour centres show greater thermal stability than organic dyes.

5.1.2. The LD-pumped Nd:YLF laser. The Nd:YLF laser has several properties very different from those of the Nd:YAG laser. The fact that it is a uniaxial material means that, simply by using an intracavity polarizer, one can select one of two different wavelengths for each transition. For the $^4F_{3/2}$–$^4I_{11/2}$ transition these wavelengths are 1.047 μm, and 1.053 μm, with the 1.047 μm polarization exhibiting the higher gain. The natural birefringence of Nd:YLF swamps the effect of thermally induced birefringence observed in materials such as Nd:YAG. Fan *et al* [69] reported the efficient diode-pumped operation of the Nd:YLF laser, where output was obtained at both 1.047 μm and 1.053 μm. For the high-gain polarization (1.047 μm), an optical slope efficiency of 38% was observed. The lower pump power threshold (<1 mW) obtained (compared with similar LD-pumped Nd:YAG lasers) can be attributed to the higher product of the stimulated emission cross section and the fluorescence lifetime for Nd:YLF (see table 1). More recently, Baer *et al* [60] obtained a TEM_{00} output power greater than 3 W using the tightly folded resonator. The highest CW output power from an LD-pumped Nd:YLF laser was obtained by Keirstead and Baer [70]. They used three 10 W LD bars as the pump source, and obtained 10 W of TEM_{00} output power. The optical slope efficiency was greater than 40%. Utano *et al* [71] side pumped an Nd:YLF laser using an LDA. The array output consisted of >100 mJ pulses of duration 300 μs. An optical slope efficiency of 42.9% was observed for long pulse operation, with a maximum output energy of 30 mJ.

The fluorescence lifetime of Nd:YLF is approximately twice as long as that of Nd:YAG. Furthermore, a large amount of energy can be stored in the medium gain 1.053 μm transition before the onset of amplified spontaneous emission. These facts make the LD-pumped Nd:YLF laser an attractive medium for the generation of high-power Q-switched pulses [60, 65, 68, 72–75]. The results of Grossman *et al* [68] show that approximately twice the pulse energy can be obtained from a Q-switched Nd:YLF laser than from a Q-switched Nd:YAG laser, due to the difference in the fluorescence lifetime for these media. The highest peak power that has been obtained to date from the LD-pumped Nd:YLF laser is 70 kW, in a pulse of duration <10 ns, by Baer *et al* [75]. In this work, a 10 W LD bar was used to pump a tightly folded Nd:YLF resonator.

5.1.3. The LD-pumped Nd:glass laser. Nd:glass is an ideal candidate for LD pumping due to its wide absorption spectrum in the region of 800 nm. Unlike, for example, the YAG host, the concentration of active ions can be very high before the onset of concentration quenching (approximately 7% Nd_2O_3 in phosphate glasses). The main disadvantage of glass as a host medium is its low thermal conductivity (0.6 $W\,m^{-1}\,K^{-1}$ for Schott LG760 phosphate glass as opposed to 11 $W\,m^{-1}\,K^{-1}$ for Nd:YAG). This makes the Nd:glass laser particularly susceptible to thermal effects, such as thermal lensing, thermally induced birefringence and thermal damage.

The first reported operation of an LD-pumped Nd:glass laser was by Kozlovsky *et al* [76]. A pump power threshold of 2 mW and a slope efficiency of 42% was obtained from a monolithic device, when pumped with a low-power single-stripe LD. Much lower slope efficiencies (9–12%) have been obtained when the Nd:glass laser has been pumped using high-power LDAs [77, 78]. Hughes *et al* [79, 80] pumped an

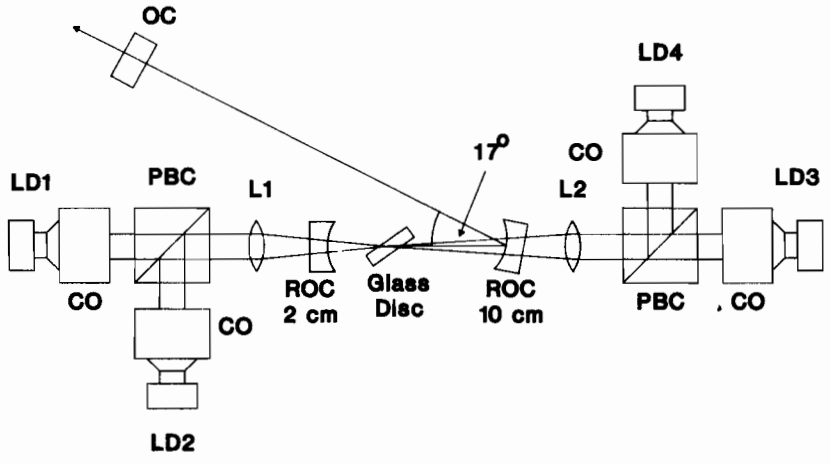

Figure 7. Schematic diagram of the high-power LD-pumped Nd:glass laser (after Hughes *et al* [80]). The abbreviations are: LD, laser diode; PBC, polarization beamsplitting cubes; CO LD, collimating optics; OC, output coupler (5% transmitting); L1, L2, spherical lenses; ROC, radius of curvature.

Nd:glass laser using a phosphate glass (Schott LG760) with two different dopings (4% wt and 8% wt). The pump sources were high-power (500 mW) broad stripe LDs. In this case, the Nd:glass laser cavity was a standard three-mirror astigmatically compensating cavity [38], and the active medium was pumped through both the cavity rear mirror and the turning mirror. This pumping scheme, shown in figure 7, was used to avoid melting the glass (this was a particular problem for the highly doped glass, where melting occurred at a pump power of about 600 mW). An output power of 420 mW was obtained at a slope efficiency of 32% [80]. The highest output power obtained from an LD-pumped Nd:glass laser was reported by Fan [81]. Using a spinning glass disc as the gain medium to overcome thermal problems, an output power of 550 mW was obtained for an absorbed power of 2 W. Basu and Byer [82] carried out an analysis of the scalability of LD-pumped Nd:glass lasers in the zig-zag slab and rotating disc geometries. They predicted that for the rotating disc laser, up to 20 kW of average output power should be achievable.

In all the above cases, the Nd:glass laser was end pumped. This laser has also been transversely pumped using pulsed LDs [54, 83]. Hanson and Imthurn [83] reported an output pulse energy of 7.5 mJ and an optical slope efficiency of 29%. The pump pulse energy was 35 mJ in 200 μs.

5.1.4. Other Nd-doped LD-pumped lasers. There have recently been several comparisons of the performance of LD-pumped Nd:YAG lasers with that of LD-pumped Nd:$La_2Be_2O_5$ (Nd:BEL) lasers [84–86]. Scheps [85] reported 635 mW output from an LD-pumped Nd:BEL laser, with an optical slope efficiency of 46%. This corresponded to an overall efficiency of 9.5%. The performance was below that of a similar Nd:YAG laser due partly to the smaller $\sigma\tau$ product, which increases the pump power threshold, and partly to the low quantum efficiency and higher internal loss of Nd:BEL. It was noted, however, that the broad absorption spectrum of Nd:BEL in the region of 800 nm may make it a superior host to Nd:YAG for pulsed high-power transverse pumping, where the LD emission spectrum tends to be larger. Rappoport and Chin [86] commented on Nd:BEL's greater energy storage capacity and its ability to be doped to higher levels than Nd:YAG.

Work reported on the LD-pumped Nd:YVO_4 laser [1, 87] has shown that this laser outperforms both Nd:YAG and Nd:BEL in terms of slope efficiency and threshold. Fields *et al* [1] reported 750 mW output power, 64% optical slope efficiency, and an overall efficiency of 15.8%. It was also noted [87] that a further advantage of Nd:YVO_4 is its broad absorption band in the 800 nm region. Its high stimulated emission cross section at 1.342 μm (similar to that of Nd:YAG at 1.064 μm) should lead to a very efficient 1.3 μm LD-pumped Nd:YVO_4 laser. Jain *et al* [88] obtained an output of 18 mW at 1.3 μm for a 200 mW pump power. The relatively high threshold pump power (50 mW) and low slope efficiency was attributed to poor polishing of the crystals used.

The LD-pumped Nd:$YAlO_3$ (Nd:YAP) laser has been operated successfully at both 1.34 μm [89] and 1.079 μm [90]. At 1.34 μm, the optical slope efficiency was 9% and the maximum output power was 26 mW. This relatively low efficiency was attributed to poor spatial overlap of the pump beam and the Nd:YAP laser mode. Schearer and Tin [90] reported an output power of over 100 mW at 1.079 μm for an incident pump power of 450 mW. By using a Lyot filter, laser emission on six of the laser lines of the $^4F_{3/2}$–$^4I_{11/2}$ transition was obtained. Of particular interest was the generation of output at 1083 nm, since this corresponds to the helium triplet resonance line. Many of the physical and spectroscopic properties of Nd:YAP are similar

to those of Nd:YAG, although YAP, like YLF, is an anisotropic material.

The helium triplet resonance line can also be accessed using the LD-pumped $La_xNd_{1-x}MgAl_{11}O_{19}$ (LNA) laser [91, 92]. One of the differences between the LNA laser and the Nd:YAG laser is the Nd concentration, which can be much higher for the LNA laser. Output powers of up to 100 mW were obtained using a 500 mW CW pump source, and the emitted wavelength could be tuned from 1.046 μm to 1.090 μm [92].

Nd-doped gadolinium scandium gallium garnet (Nd:GSGG) has been investigated [93] as a potential laser material for high average power output using LD side pumping. Much of the literature (e.g. [94]) has been concerned with Cr^{3+} sensitized GSGG. However, while the Cr^{3+} ion are useful in flashlamp-pumped systems for absorbing pump photons whose energies lie outside the Nd^{3+} absorption band, they also contribute to heating of the host material via non-radiative transitions. For LD pumping, co-sensitization with Cr^{3+} ions is not helpful, since the absorption of the relevant Cr^{3+} level ($^4T_2$) is low at 800 nm. Also, the emission of the LD source falls mainly within the Nd^{3+} absorption band. Nd:GSGG can be doped to higher levels than Nd:YAG before the onset of concentration quenching (due to its larger lattice parameter) and has a larger absorption than Nd:YAG at the peak of its absorption band (808 nm). The smaller stimulated emission cross section [95] of Nd:GSGG also means that more energy can be stored in this medium before the onset of ASE. All these factors suggest that Nd:GSGG could be a useful laser material for high average power Q-switched operation. Caffey *et al* [93] reported on optical slope efficiency of 41.5% for Nd:GSGG in the rod geometry when side pumped. They also noted that this maximum slope efficiency was observed when the pump wavelength was detuned to 811 nm, away from the maximum absorption. This was attributed to a more uniform and deeper penetration of the pump radiation into the rod.

Verdun and Thomas [96] recently reported results obtained from a new laser crystal, $Nd:CaYAlO_4$. Attractive properties of this material include its broad absorption spectrum centred at 808 nm. An output power of 80 mW was obtained for an absorbed pump power of 650 mW. The authors also observed that the thermal conductivity of this material is expected to be much larger than that of Nd:glass, so that improved thermal performance may be achieved.

The LD-pumped properties of $Nd^{3+}:Y_3Sc_2Al_3O_{12}$ (Nd:YSAG) [97] and $Nd^{3+}:Ba_2ZnGe_2O_7$ (Nd:BZAG) [98] have also recently been reported. In each case, the laser medium, which was a rod, was side pumped using a pulsed LD whose output consisted of 475 W in a variable 100–300 μs pulse. Nd:BZAG yielded an optical slope efficiency of 22.8% and Nd:YSAG 9.2%. These slope efficiencies are significantly lower than the 47.7% recorded for Nd:YAG in a similar set-up [34]. In the case of Nd:YSAG, the authors attribute the low slope efficiency to the poor optical quality of the crystal. However, they note that Nd:YSAG has an advantage over Nd:YAG as a potential material for Q-switched operation due to its longer fluorescence lifetime at high Nd^{3+} concentrations. In the case of Nd:BZAG, the authors attribute the lower slope efficiency to less efficient pump coupling due to the use of a smaller diameter rod, and higher scattering losses.

It is often required to double the frequency of the near infrared radiation obtained from Nd-doped LDPSSLs into the visible part of the spectrum. We consider self-frequency doubling where the laser crystal acts as both gain medium and nonlinear crystal. For this purpose, there is much interest in $MgO:LiNbO_3$, which is a host medium with excellent electro-optical and nonlinear properties. Self-frequency-doubled operation has been obtained in an $Nd:MgO:LiNbO_3$ laser-pumped by a dye laser at 598 nm [99]. To date, however, self-frequency-doubled operation has not been reported in this laser using diode-pumping. Cordova-Plaza *et al* [100] have obtained an optical slope efficiency of 37% from an LD-pumped $Nd:MgO:LiNbO_3$ CW laser, with an absorbed pump power threshold of 1.9 mW. There appears no obvious reason why this laser should not operate self-frequency doubled in the near future.

Self-doubled operation has been achieved in the LD-pumped $Nd_xY_{1-x}Al_3(BO_3)_4$ (Nd:YAB) laser [101, 102]. In Nd:YAB, the Nd^{3+} concentration can be much higher than in Nd:YAG without suffering quenching effects. Nd:YAB also has a higher absorption and a broader absorption spectrum (6 nm) than Nd:YAG at 800 nm. Lin *et al* [102] obtained more than 80 mW of green radiation with a pumping power of 1 W from a monolithic device. They predicted that with properly optimized coatings, 150–200 mW CW green output should be obtained using a 1 W LD-pumped laser.

5.2. Other rare earth (RE)-doped laser diode pumped lasers

We now consider the operation of LDPSSLs using transitions in RES other than neodymium. This section will be divided into three subsections, focusing on holmium-, thulium- and erbium-doped lasers.

5.2.1. The laser diode pumped Ho-doped laser. There is much interest in the 2.1 μm $^5I_7$–$^5I_8$ transition in Ho^{3+}, due to its eyesafe wavelength. Because of the three-level nature of this transition, early work required cooling to 77 K to obtain laser action [103]. In this laser, the Ho:YAG laser medium was sensitized using Er^{3+} and Tm^{3+}. The LD wavelength was temperature tuned to the centre of the Ho:YAG absorption band at 785.5 nm. A comparison carried out with Nd:YAG indicated a lower pump power threshold for Ho:YAG. This is not surprising when one considers the long fluorescence lifetime (5 ms) of Ho:YAG. Later work on the LD-pumped Ho:YAG laser [104–106] reported room-temperature operation of this laser. This was accomplished using high thulium doping compared with

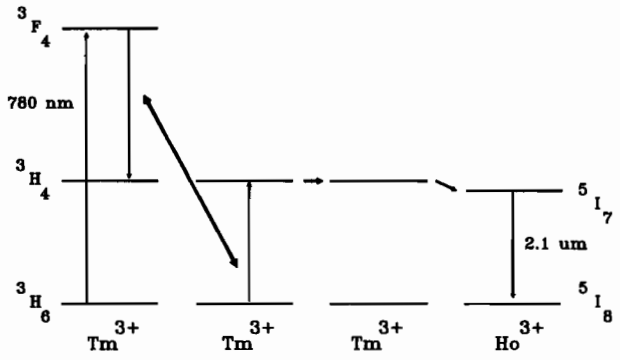

Figure 8. Cross relaxation process in the thulium-sensitized holmium laser. The pump radiation (780 nm) is absorbed by a thulium ion. There follows a cross relaxation process where two excited ($^3H_4$) thulium ions are obtained from a single pump photon. Rapid energy migration occurs among the thulium ions, followed by energy transfer to the holmium $^5I_7$ level. 2.1 μm lasing then takes place from this level.

holmium doping (16 times greater [106]) which enables effective cross relaxation to occur in the thulium ions. This cross relaxation process can result in two excited holmium ions for each 785 nm photon absorbed as shown in figure 8. The lower holmium doping also improves the laser performance by keeping reabsorption losses to a minimum. Using this cross relaxation scheme, Fan *et al* [106] reported operation of the LD-pumped Ho:YAG laser with a slope efficiency of 19% and a pump power threshold of 4.4 mW. Kane and Wallace [107] have reported output powers as high as 34 mW for a pump power of 170 mW when the Tm:Ho:YAG crystal was reduced in temperature to −55 °C.

This laser transition has also been successfully LD pumped when the host medium was YLF [108, 109]. At room temperature, Hemmati [109] reported a 30% slope efficiency and a pump power threshold of 108 mW. Both Ho:YAG and Ho:YLF appear promising candidates for Q-switched operation due to their long fluorescence lifetimes (5 ms and 12 ms respectively). Hemmati [109] reported a pulse energy of 165 μJ at a repetition rate of 100 Hz from Ho:YLF.

5.2.2. The laser diode pumped Tm laser. Also of interest in the same wavelength region as the Ho laser is the $^3F_4$–$^3H_6$ laser transition in Tm^{3+}. Kintz *et al* [110] reported 2.02 μm emission at a slope efficiency of 56% at room temperature of an LD-pumped Tm:YAG laser. The high efficiency was once again due to a cross relaxation process in the Tm^{3+} ions. More recently, Kintz [111] reported 200 mW output from an LD-pumped Tm:YAG laser. The fluorescence lifetime was measured to be between 6 and 13 ms, suggesting that Tm:YAG is a good candidate for high-energy Q-switched operation. Suni and Henderson [112] have reported both CW and Q-switched operation, obtaining CW output powers of 530 mW multimode for a pump power of 1.37 W. This corresponded to an optical slope efficiency of 49%. When Q-switched, a pulse energy of 1 mJ was obtained at a repetition rate of 100 Hz, and the output was single transverse mode. More recently, Suni and Gates [113] reported 2.5 mJ pulse energies at a repetition rate of 50 Hz.

5.2.3. Laser diode pumped Er/Yb lasers. Kintz *et al* [114] have reported both CW and pulsed operation from the 2.8 μm $^4I_{11/2}$–$^4I_{13/2}$ transition in Er:YLF. For CW operation, the pump power threshold was 147 mW and the optical slope efficiency 0.7%. The CW operation was achieved on a normally self-terminating transition, and was attributed to a cooperative upconversion process. The authors suggested that an order of magnitude increase in slope efficiency should be possible. This was achieved by Esterowitz and Stoneman [115] who obtained an optical slope efficiency of 10%. The authors noted that this increase was due to a greatly increased Er concentration (four times greater than that used by Kintz *et al* [114]). They also commented that a further increase in the Er concentration may not be useful due to a cross relaxation process from the $^4I_{9/2}$–$^4I_{13/2}$ level.

The work described thus far has concentrated on the use of LDs operating in the 800 nm region. However, the recent development of strained layer InGaAs LDs operating between 870 nm and 1.1 μm has opened the way to pumping erbium [116] and ytterbium [117] doped lasers at these longer wavelengths. Hutchinson *et al* [116] used ytterbium as a codopant in an Er:glass laser operating at 1.535 μm (the $^4I_{13/2}$–$^4I_{15/2}$ transition). The Yb^{3+} absorption was nearly at its maximum at the pump wavelength (962 nm), while Er^{3+} ESA was avoided. The optical slope efficiency obtained was 7.1% and the pump power threshold was 0.9 mJ in an end-pumped configuration. The Er^{3+} $^4I_{13/2}$ level fluorescence lifetime was measured to be 7.6 ms. The authors noted that this slope efficiency was greater than any reported previously for either flashlamp or laser pumping of Er:glass. Lacovara *et al* [117] used a strained layer InGaAs quantum well laser to diode pump a Yb:YAG laser, and obtained an optical slope efficiency as high as 25%. The authors noted that the absorption spectrum of Yb^{3+} in the emission region of these LDs is 18 nm wide, considerably broader than that of Nd:YAG, and that the fluorescence lifetime is 1.26 ms for a doping level as high as 6.5%.

5.3. Tunable laser diode pumped lasers

Visible LDs have recently been used to pump Cr-doped solid state lasers [118–120]. Using visible LDs operating in the 670–680 nm range, Scheps *et al* [118] have successfully pumped the highly tunable alexandrite ($Cr:BeAl_2O_4$) laser. The pump power threshold was 12 mW and the optical slope efficiency was 25%. This performance was similar to that obtained using a dye laser pump at the same wavelength. Scheps *et al* [119] also reported the performance of an end-pumped Cr:LiCAF laser, using a dye laser operating between

610 and 680 nm. With a pump wavelength of 670 nm, an optical slope efficiency of 37% and a threshold pump power of 49 mW was obtained. The authors noted that this laser appears to be an excellent candidate for LD pumping. LD-pumped operation has since been realized, using two 10 mW 673 nm LDs as the pump source [120].

A further development has been the use of a frequency doubled LD-pumped Nd:YAG laser to pump a CW Ti:Al_2O_3 (Ti:sapphire) laser [121]. The single frequency Ti:sapphire ring laser was tunable from 773–829 nm when pumped with 173 mW at 532 nm. Steele *et al* [122] used an LD-pumped, Q-switched, frequency-doubled Nd:YAG laser to pump a Ti:sapphire laser, obtaining a maximum pulse energy of 720 μJ at 795 nm. The laser was tunable (using three mirror sets) from 696 nm to 1000 nm (see also section 6 for pumping of Ti:sapphire lasers with Q-switched and modelocked, frequency-doubled LD pumped Nd lasers).

Doualan [123] has used an LDA to pump a colour centre laser. The centre pumped was the $(F_2^+)^*$ centre in NaF. The absorption band peaks at 870 nm and the fluorescence spectrum at 1.07 μm; 7.8 mW of output power was obtained, and the laser was tunable from 1.03 to 1.12 μm. The author comments that it should be possible to pump other colour centre lasers using LDs.

5.4. Laser diode pumped stoichiometric lasers

In this section we consider the work carried out to date on stoichiometric laser materials. The stimulus for the research into these materials is essentially to reduce the size of LDPSSLs. Stoichiometric materials are compounds which contain the lasing species, rather than hosts into which the species is doped. Due to this, the concentration of active ions can be much larger in stoichiometric materials, resulting in a shorter absorption length for the pump radiation. Most of the work reported in this field has been concerned with lithium neodymium tetraphosphate ($LiNdP_4O_{12}$) or LNP. This material has about thirty times higher neodymium concentration than Nd:YAG, and a similar stimulated emission cross section. Kubodera *et al* [124] reported the operation of an argon ion pumped miniature LNP laser in which the active medium was a 300 μm thick crystal. The authors also predicted that this laser was a good candidate for LED pumping due to small pump beam expansion over the very thin active medium. The LD-pumped operation of LNP lasers at both 1.05 μm [125] and 1.32 μm [125, 126] has since been reported. Kubodera and Otsuka [125] reported optical slope efficiencies of 18.2% (threshold 0.6 mW) at 1.05 μm and 6.5% (threshold 2.7 mW) at 1.32 μm. The low output powers obtained (2 mW at 1.05 μm and 0.5 mW at 1.32 μm) were attributed to the low pump power. Single transverse and longitudinal mode operation was achieved at all pump powers. The authors commented that the single longitudinal mode operation was probably due partly to the etalon effect of the 300 μm thick crystal and partly due to the high-density pumping used [127] (more detailed discussion of the single longitudinal mode operation of lasers will be given in section 7).

Dixon *et al* [128] have used an interesting technique to couple the pump radiation into the LNP laser mode where the crystal is placed in very close proximity to the LD output facet. Due the very short absorption length of the LNP crystal, there is no need for collimating and focusing optics to be used, as is normally the case for LDPSSLs. Using a separate output coupler, laser operation was obtained at both 1047 nm (slope efficiency 33%) and 1317 nm (slope efficiency 10%). The maximum output powers obtained were 73.5 mW and 24 mW, respectively. Using a monolithic device, 28 mW output was obtained at 1317 nm. The authors believe that the slope efficiencies reported will increase as crystal growth and fabrication techniques are improved.

5.5. Laser diode pumped waveguide lasers

In addition to bulk lasers, there is much interest in the use of LDs to pump waveguide lasers. In this section we will discuss briefly some of the most recent work on laser performance in both optical fibre waveguides and in waveguides which have been fabricated in a bulk material.

Low threshold optical fibre devices have been reported for a variety of RE ions and glass fibre hosts. The first fibre laser to be successfully pumped with an LD was the Nd-doped silica fibre laser [22]. The laser threshold was less than 1 mW, and the lasing wavelength 1.088 μm. Subsequently, LD-pumped operation of Nd-doped silica fibre lasers was reported at 0.905 μm and 1.4 μm [129], with thresholds of 4.3 mW and 6 mW respectively. The Er-doped silica fibre laser operating at 1.553 μm has also been demonstrated [130]. The pump source in this case was a 1.48 μm InGaAsP laser.

LD-pumped optical fibre lasers have also been recently demonstrated using fluorozirconate fibres as the host medium. These have included thulium-doped fibres [131, 132] operating at 2.3 μm ($^3H_4$–$^3H_5$ transition) [131] and 1.97 μm ($^3H_4$–$^3H_6$ transition) [133]. Allen and Esterowitz [131] reported a threshold of 4 mW launched into the fibre, and commented that the laser should be continuously tunable between 2.2 and 2.5 μm. Allen *et al* [133] reported the LD-pumped operation of an erbium-doped fluorozirconate fibre operating at 2.7 μm ($^4I_{11/2}$–$^4I_{13/2}$ transition). Millar *et al* [134] have reported the operation of a neodymium-doped fluorozirconate fibre laser operating at 1345 nm. Up to 30 mW of CW output power was obtained for a pump power of 120 mW, and an optical slope efficiency of 57% was reported.

In addition to optical fibre waveguides, waveguide lasers have been fabricated in bulk glasses [135, 136] and in a variety of crystals [137–141]. The work of Mwarania *et al* [135] demonstrated the low threshold powers of these devices (7.5 mW of launched pump power from a Ti:sapphire laser operating at 807 nm). Aoki *et al* [136] reported impressive output power

(150 mW) from an LD-pumped Nd:glass waveguide laser, although it should be noted that the guide radius was very large (215 μm). Field *et al* [137, 138] have reported LD-pumped operation of Nd:YAG, Nd:MgO:$LiNbO_3$ and Nd:GGG planar waveguide lasers. The threshold absorbed powers were, respectively, 8.5 mW, 17 mW and 8 mW. The Nd:GGG waveguide laser yielded 40 mW of output power [138]. An ion implantation technique was used to fabricate the waveguides. More recently, ion implanted channel waveguide laser operation has been achieved in Nd:GGG [140] and Nd:YAG. In Nd:YAG Field *et al* obtained 4 mW of output power at an optical slope efficiency of 27%. Lallier *et al* [141] have used a proton exchange technique to fabricate a channel waveguide in Nd:MgO:$LiNbO_3$, and have pumped this laser with a Styryl 9M dye laser and a single-stripe LD. With LD pumping, the Nd:MgO:$LiNbO_3$ laser output was limited to 0.3 mW. The authors attributed this low power to excess feedback into the diode from the substrate preventing efficient coupling into the waveguide.

6. Modelocked LDPSSLs

Modelocking is a well established technique for the generation of ultra-short pulses, and much work has been reported on the modelocked LDPSSL. Results obtained using two different modelocking techniques will be discussed in this section, namely active modelocking [142] and additive-pulse modelocking (APM) [143].

In active modelocking, an intra-cavity modulator is used. This can be either an acousto-optic amplitude modulator (AM modelocking) or an electro-optic phase modulator (FM modelocking). In APM, a portion of the laser output is directed into an external cavity containing some nonlinear element, typically an optical fibre. Pulse shaping then results from the coherent addition of pulses returning from the external cavity with those already circulating in the main laser cavity. The APM mechanism is particularly attractive in that it has been shown to be self-starting (i.e. no intra-cavity modulator is required to initiate the self-starting process) in a range of laser materials including Nd:YAG [144], Nd:YLF [145] and Nd:glass [146]. A further advantage is that the shortest pulse duration which can be obtained in the case of APM modelocking is inversely proportional to the laser gain bandwidth, while for active modelocking it is inversely proportional to the square root of the gain bandwidth [147]. This means that much shorter pulses can be obtained using the APM modelocking technique.

6.1. The modelocked LD-pumped Nd-doped laser

Several authors have reported the performance of modelocked LD pumped Nd:YAG lasers using AM [64, 148–150], FM [151] and APM modelocking [144, 152]. The best performance (i.e. shortest pulse duration) obtained for each type of modelocking is shown in table 2, together with the shortest pulses obtained from the modelocked LD-pumped Nd:YLF and Nd:glass lasers.

The shortest pulses were obtained using APM modelocking. The reason for the much shorter pulse duration obtained using FM as opposed to AM modelocking is not fully understood. Maker *et al* [64] combined AM modelocking and Q-switching to yield peak powers of up to 7 kW. An FM modelocked and Q-switched Nd:YAG laser yielded peak powers as high as 19 kW and, when frequency doubled, was used to modelock a dye laser by synchronous pumping [153]. The modelocked Nd:YAG laser has been efficiently frequency doubled using an external resonant cavity [152, 154], yielding conversion efficiencies as high as 61% [154]. Keen and Ferguson [150] have combined FM modelocking and Q-switching to produce pulses of 700 W peak power from an Nd:YAG laser operating at 1.3 μm. Without the Q-switching, modelocked pulses of duration 19 ps were obtained.

The broader fluorescence linewidth of Nd:YLF means that this laser medium is capable of supporting shorter pulses than the Nd:YAG laser. The LD-pumped Nd:YLF laser has been modelocked using AM [155–158], FM [159] and APM [145] techniques. In the case of Nd:YLF, the shortest pulse duration obtained using active modelocking is 7 ps. This was produced using a high-frequency (2 GHz) AM modelocker consisting of a sapphire substrate on a lithium niobate transducer [156]. Juhasz *et al* [158] used a piezoelectrically induced strain-optic (PESO) modulator to modelock an LD-pumped Nd:YLF laser, also yielding pulses of 7 ps duration. In this type of modulator, the piezoelectric material itself is used as the deflection medium [160]. The pulse duration of 1.5 ps obtained by Malcolm *et al* using APM modelocking is the shortest achieved to date from an LD-pumped Nd:YLF laser [145]. Combined Q-switching and active modelocking of the LD-pumped Nd:YLF laser has yielded peak powers as high as 15 kW (AM modelocking) [155] and 22 kW (FM modelocking) [159]. The Q-switched and FM modelocked LD-pumped Nd:YLF laser has also been used to pump a Ti:sapphire laser [161, 162]. Malcolm and Ferguson [162] obtained a maximum pulse energy of 3 μJ from the Ti:sapphire laser, which could be tuned from 705 nm to 955 nm.

The very broad fluorescence linewidth of Nd:glass makes this laser a potential source of sub-picosecond pulses. Using active modelocking techniques [77, 78, 163–165], pulses as short as 5 ps have been obtained [165]. Sub-picosecond pulses have been obtained from an APM modelocked Nd:glass laser when a krypton ion laser was used as the pump source [146]. However, due to the lower powers which have generally been available from the LD-pumped Nd:glass laser, and the existence of an intensity threshold for the onset of self-starting APM [144], self-starting APM has not yet been demonstrated in the LD-pumped Nd:glass laser. However, with the development of high-power high-efficiency LD-pumped Nd:glass lasers [80], it is

Table 2. The shortest pulses resulting from various techniques used to modelock LD-pumped Nd-doped YAG, YLF and glass.

	Nd:YAG	Nd:YLF	Nd:glass
Fluorescence linewidth (GHz)	120	360	5300
AM modelocking	55 ps [64]	7 ps [157]	5 ps [165]
FM modelocking	12 ps [151]	9 ps [73]	9 ps [78]
APM modelocking	1.7 ps [144]	1.5 ps [145]	600 fs [192]

expected that self-starting APM will be reported in the near future.

7. Single-frequency LDPSSLs

In this section we discuss the methods which have been used to obtain single-frequency (i.e. single-longitudinal and transverse mode) operation, and the various LDPSSLs to which these techniques have been applied. We will first consider standing wave resonators, both monolithic and hybrid (those where separate output couplers have been used). We will then consider the various ring laser configurations which have been used to achieve single-frequency operation.

7.1. Standing wave cavities

The simplest method of achieving single-longitudinal mode (SLM) operation of a laser is by using a short monolithic resonator. Multi-longitudinal mode operation of lasers is largely due to the phenomenon of spatial hole burning. One way of alleviating this problem is to choose a cavity length so short that only one longitudinal mode falls under the gain curve. This technique has been graphically demonstrated in Nd:YAG at both 1.06 μm [35, 36] and 1.3 μm [166, 167], and in the Ho:YAG laser operating at around 2 μm [168–170]. Zayhowski and Mooradian [35] reported successful, repeatable SLM operation of a monolithic Nd:YAG laser at pump powers of around forty times the 1 mW threshold when pumped with a Ti:sapphire laser. This corresponded to an output power of 8 mW. At higher pump powers, they commented that their results were unrepeatable due to thermal effects, although an SLM output power of 22 mW was obtained. SLM operation was also obtained using an unfocused 20 mW LD as the pump. Some of the other main results from such lasers are shown in table 3. In each case, SLM operation was observed.

For all available pump powers, Storm [168] reported that a Tm:YAG laser yielded multi-longitudinal mode operation despite using an identical resonator to that used for an SLM Ho:YAG laser. The reason for this was not fully understood.

Several authors have also reported successful SLM operation from LDPSSLs where the cavity is long enough to support several longitudinal modes [63, 171–173]. In such lasers, multi-longitudinal mode operation is obtained at pump powers not far above pump threshold, due to the onset of spatial hole burning. As an example, Zhou *et al* [171] observed a 2.3 mW threshold and a 25% slope efficiency using a monolithic, 5 mm long, Nd:YAG rod. The threshold of the second longitudinal mode occurred at an Nd:YAG output power of 1.2 mW. Scheps and Heller [173] observed an SLM output power as high as 18.6 mW for an Nd:BEL laser in a hybrid cavity. When pumped with a dye laser, an SLM power of 31 mW was obtained from this Nd:BEL laser. This was despite the fact that the longitudinal mode spacing (6 GHz) was small compared with the gain bandwidth (156 GHz). The authors commented that this was consistent with the theory of Otsuka and Kubodera [174]. In this theory, the authors show that energy diffusion in lasers, which can reduce the effects of spatial hole burning, increases with absorbed pump density.

In order to increase the SLM power obtained from standing wave cavities, the use of both gain-switching [172] and Q-switching techniques [63] have been reported. Owyoung *et al* [172] obtained 60 mW of SLM peak power by first pumping an Nd:YAG laser at its threshold level of 1.5 mW to establish SLM operation. Gain switching was then accomplished by pulsing the LD drive current significantly above its threshold value for several microseconds. Maker and Ferguson [63] established SLM operation by adjusting the radio frequency (RF) drive power to an acousto-optic Q-switch so that the Nd:YAG laser was operating just above threshold. The RF power was then switched off, and the Q-switched pulse developed out of the single mode already oscillating. Pulses of peak power 125 W and duration 40 ns were reported.

Etalons have been used in a range of LDPSSLs to obtain SLM operation [175–177] and also for frequency tuning [176, 177]. Nachman *et al* [176] used three etalons to ensure SLM operation at low output powers (~1 mW, due to a low power pump LD) and to obtain frequency tuning over ~3 THz, for an Nd:glass laser operating at 1.06 μm. Henderson and Hale [177] obtained 58 mW of SLM output power and frequency tuning over a 1 THz range from a Tm:Ho:YAG laser operating around 2.09 μm. This work was carried out at −40 °C.

7.2. Unidirectional ring lasers

The limitation on SLM output power available due to spatial hole burning in standing wave cavities may be

Table 3. Single-frequency performance of some LDPSSLS.

Laser	Wavelength (μm)	Type of cavity	Focused diode beam	Maximum SLM power (mW)
Nd:YAG [35]	1.064	Monolithic	No	22 mW (Ti: sapphire-pumped)
Nd:YAG [166]	1.3	Hybrid	Yes	10 mW
Ho:YAG [170]	2.12	Monolithic	Yes	13 mW

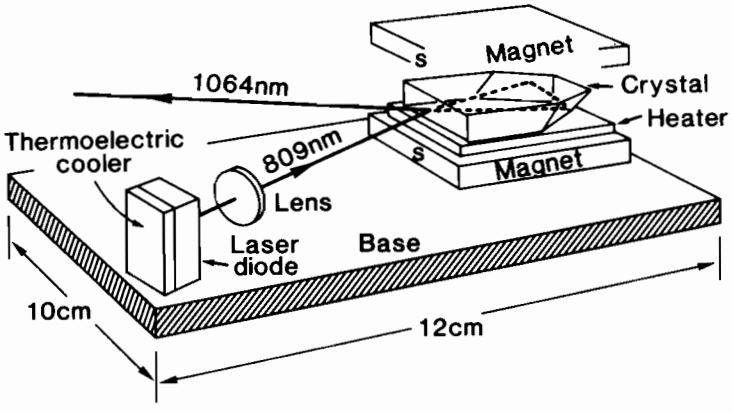

Figure 9. Schematic diagram of the non-planar ring oscillator (after Fan and Byer [6]).

alleviated by the use of a unidirectional ring laser. The ring laser cavity supports a pair of counter-propagating travelling waves rather than the standing waves of the linear cavity. To achieve SLM operation from a ring laser it is necessary to suppress one of these travelling waves. The usual method of accomplishing this involves the use of a Faraday rotator, a polarizer, and a polarization rotator. For one propagation direction, the polarization rotations produced by the Faraday rotator and the polarization rotator can be made to cancel, while for the other direction they will add. The polarizer will then allow oscillation to occur in one direction only.

It is possible to obtain unidirectional operation in an Nd:YAG ring laser by applying a magnetic field to the laser rod, utilizing its small Verdet constant. This technique was used by Scheps and Myers [178], who reported CW SLM output in excess of 540 mW, and multi-longitudinal mode Q-switched pulses of energy 22.4 μJ at a repetition rate of 5 kHz. Clarkson and Hanna [179] used a lithium niobate rhomb to define the ring path, provide the polarization discrimination and act as a Q-switch. Output pulse energies of 20 μJ were obtained at a repetition rate of 500 Hz.

A design which has recently received much attention is the non-planar ring oscillator (NPRO) [180, 181, 182]. In this device, shown in figure 9, the out-of-plane geometry provides the optical polarization required to compensate for the Faraday rotation. Once again, the laser medium acts as the Faraday rotator, and polarization discrimination is provided by non-normal incidence on the output coupler. Using an argon laser pumped Nd:YAG NPRO, Kane and Byer [180] obtained a pump-limited output of 163 mW. Cheng and Kane [181] have recently reported SLM output as high as 910 mW using a 2 W LDA to pump an NPRO. Trutna *et al* [182] used a modification of the design of Kane and Byer to obtain SLM operation of a diode-pumped Nd:YAG NPRO at 1.319 and 1.338 μm. The modification was to make the ring almost planar, which meant that a smaller magnetic field was required to enforce unidirectional operation. Due to the low-frequency noise of the LD pumps, and the monolithic design of these devices, the free-running NPRO show excellent short-term frequency stability (3–10 kHz) [183, 184]. NPROs have also been very successfully actively frequency stabilized for long-term operation [185].

The Faraday effect is not the only technique which has been used to enforce unidirectional operation. Bromley and Hanna [186] used an acousto-optic modulator both to enforce unidirectional operation of a ring laser and to act as a Q-switch. It was found that an RF drive power of only 250 mW was required to cause unidirectional operation. The mechanism by which the modulator enforces unidirectional operation is not fully understood. Pulses of energy 13 μJ and duration 36 ns were obtained, at a repetition rate of 1 kHz. Using a rhomb-type ring laser design shown in figure 10, Clarkson and Hanna obtained acousto-optically induced SLM operation of both the Nd:YAG laser [187] and the

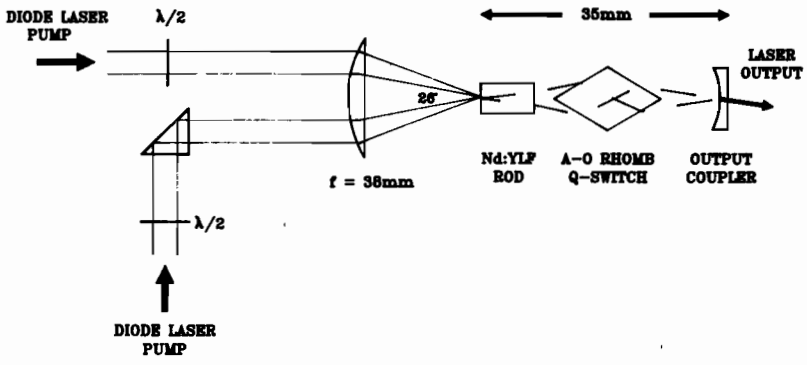

Figure 10. Schematic diagram of the LD-pumped Nd:YLF ring laser configuration where an acousto-optic modulator has been used to induce single-frequency operation (after Clarkson and Hanna [188]).

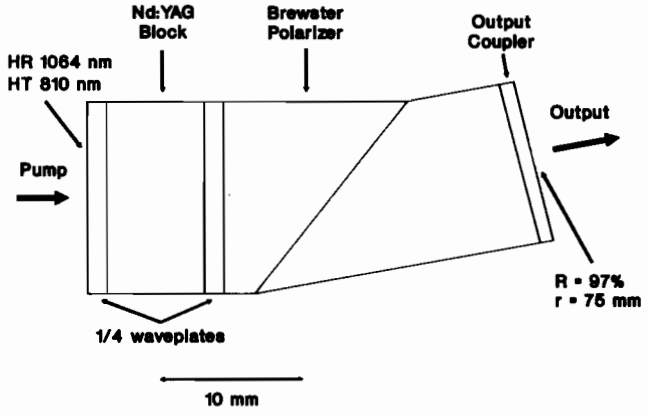

Figure 11. Schematic diagram of the monolithic twisted mode cavity Nd:YAG laser (after Wallmeroth [190]).

Nd:YLF laser [188]. Q-switched peak powers of 1 kW (Nd:YAG) and 6 kW (Nd:YLF) were observed.

7.3. The twisted mode cavity laser

The use of a twisted mode cavity (TMC) laser to obtain single frequency operation was first reported by Evtuhov and Siegman [189]. In the TMC laser, two quarter-wave plates are used, one on either side of the gain medium. If the axes of the wave plates are properly adjusted, a standing wave with an axially uniform energy density can be created. Spatial hole burning is thus eliminated. Wallmeroth [190] has reported the use of a diode-pumped twisted mode cavity Nd:YAG laser to produce SLM operation. Using a monolithic TMC design as shown in figure 11, Wallmeroth obtained an SLM output of 80 mW. A linewidth of below 10 kHz was measured for the free-running device. Using a non-monolithic design, Wallmeroth and Peuser [191] had earlier reported 255 mW of single-frequency output from a TMC laser.

8. Conclusion

The LDPSSL has progressed spectacularly during the last six years. All areas of the relevant technology have improved. Average powers from CW devices are approaching the level previously associated with arc pumped systems. Single-frequency operation, which is an area not normally associated with traditional solid state devices except for very specialized applications, has continually improved in terms of linewidth, stability and delivered power. Modelocked operation has undergone a large change in pulse duration from typically 50–100 ps from an actively modelocked lamp pumped system to around 2 ps from APM modelocked LDPSSLs. As one example of the speed of progress in this field, preliminary results have demonstrated subpicosecond pulses from an LD-pumped APM Nd:glass laser [192]. Wavelength diversity is continually being addressed in two ways. Different dopant materials and hosts are being tested and evaluated. Alternatively, nonlinear processes are being utilized to provide tunable radiation. A synchronously pumped tunable parametric oscillator has been recently demonstrated which provides 2 ps pulses over a 92 nm range around 1.047 μm, although a significantly larger range is possible in an optimized system [193].

The improvements in the LD pump source that made this field possible are continuing. The major benefit of price reductions in the cost of LDs is to make LDPSSLs competitive with traditional systems. Continual

improvements to wavelength coverage, lifetime and output power may be expected.

The activity and growth in this field make the writing of a review such as this difficult. Reports of interesting experiments which should be included appear monthly. Important areas, for example second harmonic generation using LDPSSLs, have only been mentioned indirectly. The maturity and level of activity in the LDPSSL field make the scope of this review similar to attempting to review the complete solid state laser research area.

Acknowledgments

This work has been partially supported by the following: the Science and Engineering Research Council under grant number GR/F 40658, the Department of Physics and Optoelectronics Research Centre, Southampton University and the Nuffield Foundation. DWH gratefully acknowledges financial support from the SERC.

References

[1] Fields R A, Birnbaum M and Fincher C L 1988 15.8% efficient diode laser end pumped Nd:YVO_4 laser *Tech. Dig. CLEO (Anaheim, CA)* paper PD3

[2] Streifer W, Scifres D R, Haragel G L, Welch D F, Berger J and Sakamoto M 1988 Advances in diode laser pumps *IEEE J. Quant. Electron.* **24** 883

[3] Newman R 1963 Excitation of Nd fluorescence in $CaWO_4$ by recombination radiation in GaAs *J. Appl. Phys.* **34** 437

[4] Ross M 1968 YAG laser operation by semiconductor laser pumping *Proc. IEEE* **56** 196

[5] Allen R B and Scalise S J 1969 Continuous operation of a YAlG:Nd laser by injection luminescent pumping *Appl. Phys. Lett.* **14** 188

[6] Fan T Y and Byer R L 1988 Diode laser pumped solid state lasers *IEEE J. Quant. Electron.* **24** 895

[7] Keynes R J and Quist T M 1964 Injection luminescent pumping of CaF_2U^{3+} with GaAs diode lasers *Appl. Phys. Lett.* **4** 50

[8] Ochs S A and Pankove J I 1964 Injection-luminescence pumping of CaF_2:Dy^{2+} *Proc. IEEE* **52** 182

[9] Johnson L J and Nassau N 1961 Infrared fluorescence and stimulated emission of Nd^{3+} in $CaWO_4$ *Proc. IRE* **49** 1704

[10] Geusic J E, Marcos H M and van Uitert L G 1964 Laser oscillation in Nd doped yttrium aluminium, yttrium gallium gallium, and gadolinium garnets *Appl. Phys. Lett.* **4** 182

[11] Rosencrantz L J 1973 GaAs diode pumped Nd:YAG laser *J. Appl. Phys. Lett.* **43** 4603

[12] Chesler R B and Draegert D A 1973 Miniature diode pumped Nd:YAlG lasers *Appl. Phys. Lett.* **23** 235

[13] Draegart D A 1973 Single diode end pumped Nd:YAG laser *IEEE J. Quant. Electron.* **9** 1146

[14] Chesler R B and Singh S 1973 Performance model for end pumped miniature Nd:YAlG lasers *J. Appl. Phys.* **44** 5441

[15] Koester C J 1966 Laser action by enhanced total internal reflection *IEEE J. Quant. Electron.* **2** 580

[16] Koester C J and Snitzer E 1964 Amplification in a fibre laser *Appl. Opt.* **3** 1182

[17] Stone J and Burrus C A 1974 Neodymium doped fibre lasers—room-temperature CW operation with an injection laser pump *Appl. Opt.* **13** 1256

[18] Stone J, Burrus C A, Dentai A G and Millar B I 1976 Nd:YAG single crystal fibre lasers—room-temperature operation using a single LED as a pump *Appl. Phys. Lett.* **29** 37

[19] Burrus C A, Stone J and Dentai A G 1976 Room-temperature 1.3 μm operation of a glass clad Nd:YAG single crystal fibre laser end pumped with a single LED *Electron. Lett.* **12** 600

[20] Stone J and Burrus C A 1979 Self contained LED pumped single crystal Nd:YAG fibre laser *Fibre Int. Opt.* **2** 19

[21] Poole S B, Payne D N and Ferman M 1985 Fabrication of low loss optical fibres containing rare earth ions *Electron. Lett.* **21** 738

[22] Mears R J, Reekie L, Poole S B and Payne D N 1985 Neodymium doped silica single mode fibre lasers *Electron. Lett.* **21** 738

[23] Jauncey I M, Lin J T, Reekie L and Mears R J 1986 An efficient diode pumpable CW and Q-Switched single mode fibre lasers *Electron Lett.* **22** 198

[24] Mears R J, Reekie L, Jauncey I M, Poole S B and Payne D N 1987 Diode pumped operation of an erbium doped single mode fibre laser *Electron. Lett.* **23** 1076

[25] Norrie C J, Sinclair B D, Gallaher N, Sibbett W and Dunn M H 1989 Measurement of frequency sweep in a quasi-CW diode-laser array, and its implications for pumping solid-state lasers *J. Mod. Optics.* **36** 1

[26] Forkner J F and Kuntz D W 1983 Characteristics of efficient laser diode collimators *SPIE* **390**

[27] Kuntz D W 1984 Specifying laser diode optics *Laser Focus* **20** 44

[28] Hanna D C, Karkkainen P A and Wyatt R 1971 A simple beam expander for frequency narrowing of dye lasers *Opt. Quant. Electron.* **7** 115

[29] Duarte F J and Piper J A 1982 Dispersion theory of multiple prism beam expanders for pulsed dye lasers *Opt. Commun.* **43** 303

[30] Barr J R M 1984 Achromatic prism beam expanders *Opt. Commun.* **51** 41

[31] Duarte F J 1989 Ray transfer matrix analysis of multiple-prism dye laser oscillators *Opt. Quant. Electron.* **21** 47

[32] Kasuya T, Suzuki T and Shimoda K 1978 A prism anamorphic system for Gaussian beam expander *Appl. Phys.* **17** 131

[33] Reed M K, Kozovsky W J, Byer R L, Harnagel G L and Cross P S 1988 Diode-laser-array-pumped neodymium slab oscillators *Opt. Lett.* **13** 204

[34] Allik T A, Hovis W W, Caffey D P and King V 1989 Efficient diode-array-pumped Nd:YAG and Nd:Lu:YAG lasers *Opt. Lett.* **14** 116

[35] Zayhowski J J and Mooradian A 1989 Single frequency microchip lasers *Opt. Lett.* **14** 24

[36] Zayhowski J J and Mooradian A 1989 Frequency modulated Nd:YAG microchip lasers *Opt. Lett.* **14** 618

[37] *Product Catalog* 1991 Spectra Diode Laboratories

[38] Kogelnik H W, Ippen E P, Dienes A and Shank C V 1972 Astigmatically compensated cavities for CW dye lasers *IEEE J. Quant. Electron.* **8** 373

[39] Alfrey A J 1989 Modelling of longitudinally pumped CW Ti: Sapphire laser oscillators *IEEE J. Quant. Electron.* **25** 760

[40] Hansch T W 1989 Repetitively pulsed tunable dye laser for high resolution spectroscopy *Appl. Opt.* **11** 760
[41] Clarkson W A and Hanna D C 1988 Effects of transverse mode profile on slope efficiency and relaxation oscillations in a longitudinal pumped laser *J. Mod. Opt.* **36** 483
[42] Fan T Y, Sanchez A and DeFeo W E 1989 Scalable, end-pumped, diode-laser-pumped laser *Opt. Lett.* **14** 1057
[43] Berger J, Welch D F, Streifer W, Scifres D R, Hoffman N J, Smith J J and Radecki D 1988 Fibre-bundle coupled, diode end-pumped Nd:YAG laser *Opt. Lett.* **13** 306
[44] Sipes D L 1985 Highly efficient neodymium:ytterbium aluminium garnet laser end pumped by a semiconductor laser array *Appl. Phys. Lett.* **47** 74
[45] Berger J, Welch D F, Scifres D R, Streifer W and Cross P S 1987 High power, high efficiency neodymium:ytterbium aluminium garnet laser end pumped by a laser diode array *Appl. Phys. Lett.* **51** 1212
[46] Shannon D C and Wallace R W 1991 High-power Nd:YAG laser end pumped by a CW, 10 mm × 1 μm aperture, 10 W laser-diode bar *Opt. Lett.* **16** 318
[47] Tidwell S C, Seamans J F, Hamilton C E, Muller C H and Lowenthal D D 1991 Efficient 15 W output power, diode-end-pumped Nd:YAG laser *Opt. Lett.* **16** 584
[48] Yamaguchi S and Imai H 1991 Array laser-diode end-pumped Nd:YAG laser *Tech. Dig. CLEO'91 (Baltimore, MD)* Paper CFC6
[49] Fan T Y and Byer R L 1987 Continuous-wave operation of a room-temperature, diode-laser-pumped 946 nm Nd:YAG laser *Opt. Lett.* **12** 809
[50] Risk W P and Lenth W 1987 Room-temperature, continuous-wave, 946 nm Nd:YAG laser pumped by laser-diode arrays and intracavity frequency doubling to 473 nm *Opt. Lett.* **12** 993
[51] Kozlovsky W J and Risk W P 1991 Efficient diode-laser pumped 946 nm Nd:YAG laser with resonantly enhanced pump absorption *Tech. Dig, CLEO'91 (Baltimore, MD)* Paper CME1
[52] Cuthbertson J P and Dixon G J 1991 Pump-resonant excitation of the 946 nm Nd:YAG laser *Opt. Lett.* **16** 396
[53] Fan T Y and Byer R L 1987 Modelling and CW operation of a quasi-three-level 946 nm Nd:YAG laser *IEEE J. Quant. Electron.* **23** 605
[54] Reed M K, Kozlovsky W J, Byer R L, Harnagal G L and Cross P S 1988 Diode-laser-array-pumped neodymium slab oscillators *Opt. Lett.* **13** 204
[55] Hanson F and Haddock D 1988 Laser diode side pumping of neodymium laser rods *Appl. Opt.* **27** 80
[56] Hays A D, Burnham R and Harnagel G L 1989 High-efficiency diode-array side-pumped neodymium lasers *Tech. Dig. CLEO'89 (Baltimore, MD)* Paper PD9
[57] Berger J, Harnagel G, Welch D F, Scifres D R and Streifer W 1988 Direct modulation of a Nd:YAG laser by combined side and end laser diode pumping *Appl. Phys. Lett.* **53** 268
[58] Krebs D 1987 *Laser Focus* **23** 6
[59] Burnham R and Hays A D 1989 High-power diode-array-pumped frequency-doubled CW Nd:YAG laser *Opt. Lett.* **14** 27
[60] Baer T M, Head D F and Sakamoto M 1989 High efficiency diode-bar pumped solid state laser using a tightly folded resonator *Tech. Dig. CLEO'89 (Baltimore, MD)* Paper FJ5
[61] Watanabe S, Kudo S, Yamane T and Washio K 1989 Efficient and high-power Nd:YAG laser multiple-facet end pumped by laser diodes *Tech. Dig. CLEO'89 (Baltimore, MD)* Paper PD8
[62] Pfistner C, Albers P and Weber H P 1990 Efficient Nd:YAG slab longitudinally pumped by diode lasers *IEEE J. Quant. Electron.* **26** 827
[63] Maker G T and Ferguson A I 1988 Single-frequency Q-switched operation of a laser-diode-pumped Nd:YAG laser *Opt. Lett.* **13** 461
[64] Maker G T, Keen S J and Ferguson A I 1988 Mode-locked and Q-switched operation of a diode laser pumped Nd:YAG laser operating at 1.064 μm *Appl. Phys. Lett.* **53** 1675
[65] Linne M and Baer T 1988 Q-switching of diode-pumped solid state lasers *Proc. SPIE* **898** 110
[66] Gerstenberger D C, Drobshoff A and Wallace R W 1990 High-peak-power operation of a diode-pumped Q-switched Nd:YAG laser *Opt. Lett.* **15** 124
[67] Morris J A and Pollock C R 1990 Passive Q switching of a diode-pumped Nd:YAG laser with a saturable absorber *Opt. Lett.* **15** 440
[68] Grossman W M, Gifford M and Wallace R W 1990 Short-pulse Q-switched 1.3- and 1-μm diode-pumped laser *Opt. Lett.* **15** 622
[69] Fan T Y, Dixon G J and Byer R L 1986 Efficient GaAlAs diode-laser-pumped operation of Nd:YLF at 1.047 μm with intracavity frequency doubling *Opt. Lett.* **11** 204
[70] Keirstead M S and Baer T M 1991 10 W, TEM_{00} output from a diode-pumped, solid-state laser *Tech. Dig. CLEO'91 (Baltimore, MD)* Paper CFC3
[71] Utano R A, Hyslop D A and Allik T H 1990 Diode array side-pumped Nd:$YLiF_4$ laser in solid state lasers *Proc. SPIE* **1223** 128
[72] Maker G T and Ferguson A I 1989 Mode-locking and Q-switching of a diode laser pumped neodymium-doped yttrium lithium fluoride laser *Appl. Phys. Lett.* **54** 403
[73] Maker G T and Ferguson A I 1989 Frequency modulation mode-locking and Q-switching of diode-laser-pumped Nd:YLF laser *Electron. Lett.* **25** 1025
[74] Zbinden H and Balmer J E 1990 Q-switched Nd:YLF laser end pumped by a diode-laser bar *Opt. Lett.* **15** 1014
[75] Baer T M, Head D F and Gooding P 1990 High peak power Q-switched Nd:YLF laser using a tightly folded resonator *Tech. Dig. CLEO'90 (Anaheim, CA)* Paper CMF2
[76] Kozlovsky W J, Fan T Y and Byer R L 1986 Diode-pumped continous wave Nd:glass laser *Opt. Lett.* **11** 788
[77] Krausz F, Brabec T, Wintner E and Schmidt A J 1989 Mode-locking of a continuous wave Nd:glass laser pumped by a multistripe diode laser *Appl. Phys. Lett.* **55** 2386
[78] Hughes D W, Barr J R M and Hanna D C 1991 Mode-locking of a diode-laser-pumped Nd:glass laser by frequency modulation *Opt. Lett.* **16** 147
[79] Hughes D W, Barr J R M and Hanna D C 1991 A high power, high efficiency, laser-diode-pumped continuous wave miniature Nd:glass laser *Opt. Commun.* **84** 401
[80] Hughes D W, Barr J R M and Hanna D C 1991 A high efficiency, laser-diode-pumped continuous wave miniature Nd:glass laser *Tech. Dig. CLEO'91 (Baltimore, MD)* Paper CME6

[81] Fan T Y 1990 Solid-state lasers pumped by advanced diode laser sources *Tech. Dig. OSA Annual Meeting (Boston, MA) 1990* Paper TVV4
[82] Basu S and Byer R L 1990 Average power limits of diode laser-pumped solid state lasers *Appl. Opt.* **29** 1765
[83] Hanson F and Imthurn G 1988 Efficient laser diode side pumped neodymium glass slab laser *IEEE J. Quant. Electron.* **24** 1811
[84] Scheps R, Myers J, Schimitschek E J and Heller D F 1988 End-pumped Nd:BEL laser performance *Opt. Eng.* **27** 830
[85] Scheps R 1989 Efficient laser diode pumped Nd lasers *Appl. Opt.* **28** 89
[86] Rappoport W R and Chin T 1989 Laser and laser related characteristics of Nd:BEL. High power and solid state lasers II *Proc. SPIE* **1040** 19
[87] Fields R A, Birnbaum M and Fincher C L 1987 Highly efficient Nd:YVO_4 diode-laser end-pumped laser *Appl. Phys. Lett.* **51** 1885
[88] Jain R K, Sipes D L, Pier T J and Hulse G R 1988 Diode-pumped 1.3 μm Nd:YVO_4 laser *Tech. Dig. CLEO'88 (Anaheim, CA)* Paper THB5
[89] Scarl D, Burnham R, Bowman S R and Feldman D J 1988 Diode-pumped 1.34 μm Nd^{3+}:$YAlO_3$ laser *Appl. Opt.* **27** 5005
[90] Schearer L D and Tin P 1989 Laser performance and tuning characteristics of a diode-pumped Nd:$YAlO_3$ laser at 1083 nm *Opt. Commun.* **71** 170
[91] Hamel J, Cassimi A, Abu-safia H, Leduc M and Schearer L D 1987 Diode pumping of LNA lasers for helium optical pumping *Opt. Commun.* **63** 114
[92] Aubert J J, Wyon Ch, Cassimi A, Hardy V and Hamel J 1989 Un laser solide accordable pompe par diode *Opt. Commun.* **69** 299
[93] Caffey D P, Utano R A and Allik T H 1990 Diode array side-pumped neodymium-doped gadolinium scandium gallium garnet rod and slab lasers *Appl. Phys. Lett.* **56** 808
[94] Caird J A, Shinn M D, Kirchoff T A, Smith L K and Wilder R E 1986 Measurements of losses and lasing efficiency in GSGG:Cr, Nd and YAG:Nd laser rods *Appl. Opt.* **25** 4294
[95] Krupke W F, Shinn M D, Marion J E, Caird J A and Stokowski S E 1986 Spectroscopic, optical and thermomechanical properties of neodymium and chromium-doped gadolinium scandium gallium garnet *J. Opt. Soc. Am.* **B3** 102
[96] Verdun H R and Thomas L M 1990 Nd:$CaYAlO_4$—a new crystal for solid-state lasers emitting at 1.08 μm *Appl. Phys. Lett.* **56** 608
[97] Allik T H, Morrison C A, Gruber J B and Kotka M R 1990 Crystallography, spectroscopic analysis, and lasing properties of Nd^{3+}:$Y_3Sc_2Al_3O_{12}$ *Phys. Rev.* B **41** 21
[98] Allik T H, Ferry M J, Reeves R J, Powell R C, Hovis W W, Caffey D P, Utano R A, Merkle L and Campana C F 1990 Crystallography, spectroscopic analysis and lasing properties of Nd^{3+}:$Ba_2ZnGe_2O_7$ *J. Opt. Soc. Am.* **B7** 1190
[99] Fan T Y, Cordova-Plaza A, Digonnet M J F, Byer R L and Shaw H J 1986 Nd:MgO:$LiNbO_3$ spectroscopy and laser devices *J. Opt. Soc. Am.* **B3** 140
[100] Cordova-Plaza A, Fan T Y, Digonnet M J F, Byer R L and Shaw H J 1988 Nd:MgO:$LiNbO_3$ continuous-wave laser pumped by a laser diode *Opt. Lett.* **13** 209
[101] Schutz I, Freitag I and Wallenstein R 1990 Miniature self-frequency-doubled CW Nd:YAB laser pumped by a diode laser *Opt. Commun.* **77** 221
[102] Lin J T, Hwang M Y and Rowe S 1990 Close-coupled diode-pumped NYAB green laser *Tech. Dig. OSA Annual Meeting (Boston, MA) 1990* Paper PDP26
[103] Allen R, Esterowitz L, Goldberg L, Weller J F and Storm M 1986 Diode-pumped 2 μm holmium laser *Electron. Lett.* **22** 947
[104] Kintz G J, Esterwitz L and Allen R 1987 CW diode-pumped Tm^{3+}, Ho^{3+}:YAG 2.1 μm room-temperature laser *Electron. Lett.* **23** 616
[105] Fan T Y, Huber G and Byer R L 1987 Continuous-wave operation at 2.1 μm of a diode-laser-pumped, Tm-sensitized Ho:$Y_3Al_5O_{12}$ laser at 300 K *Opt. Lett.* **12** 678
[106] Fan T Y, Huber G, Byer R L and Mitzscherlich P 1988 Spectroscopy and diode-laser-pumped operation of Tm,Ho:YAG *IEEE J. Quant. Electron.* **24** 924
[107] Kane T J and Wallace R W 1988 Performace of a diode-pumped Tm:Ho:YAG laser at temperatures between −55 and +20 °C *Tech. Dig. CLEO'88 (Anaheim, CA)* Paper FB3
[108] Hemmati H 1987 Efficient holmium:ytterium lithium fluoride laser longitudinally pumped by a semiconductor laser array *Appl. Phys. Lett.* **51** 564
[109] Hemmati H 1989 2.07 μm CW diode-laser-pumped Tm,Ho:$YLiF_4$ room-temperature laser *Opt. Lett.* **14** 435
[110] Kintz G J, Allen R and Esterowitz L 1988 Continuous wave laser emission at 2.02 μm from diode-pumped Tm^{3+}:YAG at room temperature *Tech. Dig. CLEO'88 (Anaheim, CA)* Paper FB2
[111] Kintz G J 1990 Highly efficient CW 2 μm laser *Tech. Dig. OSA Annual Meeting (Boston, MA) 1990* Paper ThL2
[112] Suni P J M and Henderson S W 1991 1 mJ/pulse Tm:YAG laser pumped by a 3 W diode laser *Opt. Lett.* **16** 817
[113] Suni P J M and Gates G H 1991 Damage-free operation of a 2.5 mJ Tm:YAG laser pumped by a 3 W room-temperature diode laser *Tech. Dig. CLEO'91 (Baltimore, MD)* Paper CPDP12
[114] Kintz G J, Allen R and Esterowitz L 1987 CW and pulsed 2.8 μm laser emission from diode-pumped Er^{3+}:$LiYF_4$ at room temperature *Appl. Phys. Lett.* **50** 1553
[115] Esterowitz L and Stoneman R 1989 Diode pumped Er:$LiYF_4$ CW laser at 2.8 μm with 10% slope efficiency. High power and solid state laser II *Proc. SPIE* **1040** 99
[116] Hutchinson J A, Caffey D P, Schaus C F and Trussel C W 1990 Diode pumped eyesafe erbium glass laser *Tech. Dig. CLEO'90 (Anaheim, CA)* Paper CPDP19
[117] Lacovara P, Wang C A, Choi H K, Aggarwal R I and Fan T Y 1991 Room-temperature InGaAs diode-pumped Yb:YAG laser *Opt. Lett.* **16** 1089
[118] Scheps R, Gately B M, Myers J F, Krasinski J S and Heller D F 1990 Alexandrite laser pumped by semiconductor lasers *Appl. Phys. Lett.* **56** 2288
[119] Scheps R, Myers J F and Payne S A 1990 CW and Q-switched operation of a low threshold Cr^{3+}:$LiCaAlF_6$ laser *IEEE Photon. Tech. Lett.* **2** 626
[120] Scheps R 1991 Diode pumped Cr^{3+}:$LiCaAlF_6$ laser *Tech. Dig. CLEO'91 (Baltimore, MD)* Paper CME3
[121] Harrison J, Finch A, Rines D M, Rines G A and Moulton P F 1991 Low-threshold, CW, all-solid-state Ti:Al_2O_3 laser *Opt. Lett.* **16** 581
[122] Steele T R, Gerstenberger D C, Drobshoff A and Wallace R W 1991 Broadly tunable high-power

operation of an all-solid-state titanium-doped sapphire laser system *Opt. Lett.* **16** 399
[123] Doualan J J 1989 Colour centre laser pumped by a laser diode *Opt. Commun.* **70** 225
[124] Kubodera K, Otsuka K and Miyazawa S 1979 Stable $LiNdP_4O_{12}$ miniature laser *Appl. Opt.* **18** 884
[125] Kubodera K and Otsuka K 1979 Efficient $LiNdP_4O_{12}$ laser pumped with a laser diode *Appl. Opt.* **18** 3882
[126] Kubodera K and Noda J 1982 Pure single-mode $LiNdP_4O_{12}$ solid-state transmitter for 1.3 μm fiber-optic communications *Appl. Opt.* **21** 3466
[127] Otsuka K and Kubodera K 1980 Effects of high density pumping on relaxation oscillations and mode spectra in lasers *IEEE J. Quant. Electron.* **16** 419
[128] Dixon G J, Lingvay L S and Jarman R H 1989 Lithium neodymium tetraphosphate lasers pumped via close-coupling to high-power laser diode arrays *IEEE Photon. Tech. Lett.* **1** 97
[129] Po H, Hakimi F, Mansfield R J, Tumminelli R P, McCollum B C and Snitzer E 1986 Neodymium fibre lasers at 0.905, 1.06 and 1.4 μm *J. Opt. Soc. Am.* **A3** 103
[130] Nakazawa M, Kimura Y and Suzuki K 1989 Efficient Er^{3+}-doped optical fibre amplifier pumped by a 1.48 μm InGaAsP laser diode *Appl. Phys. Lett.* **54** 295
[131] Allen R and Esterowitz L 1989 CW diode pumped 2.3 μm fiber laser *Appl. Phys. Lett.* **55** 721
[132] Carter J N, Smart R G, Hanna D C and Tropper A C 1990 CW diode-pumped operation of 1.97 μm thulium doped fluorozirconate fibre laser *Electron. Lett.* **26** 599
[133] Allen R, Esterowitz L and Ginther R J 1990 Diode-pumped single-mode fluorozirconate fibre laser from the $^4I_{11/2}$–$^4I_{13/2}$ transition in erbium *Appl. Phys. Lett.* **56** 1635
[134] Millar C A, Fleming S C, Brierly M C and Hunt M H 1990 Single transverse mode operation at 1345 nm wavelength of a diode laser pumped neodymium ZBLAN multimode fiber laser *IEEE Photon. Tech. Lett.* **2** 415
[135] Mwarania E K, Reekie L, Wang J and Wilkinson J S 1990 Low-threshold monomode ion-exchanged waveguide lasers in neodymium-doped BK-7 glass *Electron. Lett.* **26** 1317
[136] Aoki H, Maruyana O and Asahara Y 1990 Glass waveguide laser, *IEEE Photon. Tech. Lett.* **2** 459
[137] Field S J, Hanna D C, Large A C, Shepherd D P, Tropper A C, Chandler P J, Feng X Q, Townsend P D and Zhang L 1991 Ion-implanted crystal waveguide lasers *Tech. Dig. ASSL'91 (Hilton Head, SC)* Paper WF3
[138] Field S J, Hanna D C, Large A C, Shepherd D P, Tropper A C, Chandler P J, Townsend P D and Zhang L 1991 An efficient, diode-pumped, ion implanted Nd:GGG planar waveguide laser *Opt. Commun.* **86** 161
[139] Field S J, Hanna D C, Shepherd D P, Tropper A C, Chandler P J, Townsend P D and Zhang L 1992 Ion implanted Nd:YAG crystal waveguide lasers *IEEE J. Quant. Electron.* **27** 428
[140] Field S J, Hanna D C, Large A C, Shepherd D P, Tropper A C, Chandler P J, Townsend P D and Zhang L 1992 An ion implanted Nd:GGG channel waveguide laser *Opt. Lett.* To be published
[141] Lallier E, Pocholle J P, Papuchon M, de Micheli M, Li M J, He Q, Ostrowsky D B, Grezes-Besset C and Pelletier E 1990 Nd:MgO:$LiNbO_3$ waveguide laser and amplifier *Opt. Lett.* **15** 682
[142] Siegman A E and Kuizenga D J 1974 Active mode-coupling phenomena in pulsed and continuous lasers *Opto-electron* **6** 43
[143] Mark J, Lin L Y, Hall K L, Haus H A and Ippen E P 1989 Femtosecond pulse generation in a laser with a non-linear external resonator *Opt. Lett.* **14** 48
[144] Gooberlet J, Jacobson J, Fujimoto J G, Schulz P A and Fan T Y 1990 Self-starting additive-pulse mode-locked diode-pumped Nd:YAG laser *Opt. Lett.* **15** 504
[145] Malcolm G P A, Curley P F and Ferguson A I 1990 Additive-pulse mode-locking of a diode-pumped Nd:YLF laser *Opt. Lett.* **15** 1303
[146] Krausz F, Spielmann Ch, Brabec T, Wintner E and Schmidt A J 1990 Self-starting additive-pulse mode locking of a Nd:glass laser *Opt. Lett.* **15** 1082
[147] Kuizenga D J and Siegman A E 1970 FM and AM mode locking of the homogeneous laser—Part 1: Theory *IEEE J. Quant. Electron.* **6** 694
[148] Dimmick T E 1989 Semiconductor-laser-pumped, mode-locked, and frequency-doubled Nd:YAG laser *Opt. Lett.* **14** 677
[149] Walker S J, Avramopoulos H and Sizer T III 1990 Compact mode-locked solid-state lasers at 0.5- and 1-GHz repetition rates *Opt. Lett.* **15** 1070
[150] Keen S J and Ferguson A I 1989 Subpicosecond pulse generation from an all solid-state laser *Appl. Phys. Lett.* **55** 2164
[151] Maker G T and Ferguson A I 1989 Frequency-modulation mode-locking of a diode-pumped Nd:YAG laser *Opt. Lett.* **14** 788
[152] McCarthy M J, Maker G T and Hanna D C 1991 Efficient frequency doubling of a self-starting additive-pulse mode-locked diode pumped Nd:YAG laser *Opt. Commun.* **82** 327
[153] Maker G T and Ferguson A I 1989 Synchronously pumped mode-locked dye laser pumped by a frequency-doubled mode-locked and Q-switched diode laser pumped Nd:YAG laser *Appl. Phys. Lett.* **55** 525
[154] Maker G T and Ferguson A I 1990 Efficient frequency doubling of a diode-laser-pumped mode-locked Nd:YAG laser using an external resonant cavity *Opt. Commun.* **76** 369
[155] Maker G T and Ferguson A I 1989 Mode locking and Q-switching of a diode laser pumped neodymium-doped yttrium lithium fluoride laser *Appl. Phys. Lett.* **54** 403
[156] Keller U, Li K D, Khuri-Yakub B T, Bloom D M, Weingarten K J and Gerstenberger D C 1990 High-frequency acousto-optic mode-locker for picosecond pulse generation *Opt. Lett.* **15** 45
[157] Weingarten K J, Shannon D C, Wallace R W and Keller U 1990 Two-gigahertz repetition-rate, diode-pumped, mode-locked Nd:YLF laser *Opt. Lett.* **15** 962
[158] Juhasz T, Lai S T and Pessot M A 1990 Efficient short-pulse generation from a diode-pumped Nd:YLF laser with a piezoelectrically induced diffraction modulator *Opt. Lett.* **15** 1458
[159] Maker G T and Ferguson A I 1989 Frequency modulation mode-locking and Q-switching of a diode-laser-pumped Nd:YLF laser *Electron. Lett.* **25** 1025
[160] Turi L, Kuti Cs and Krausz F 1990 Piezoelectrically induced diffraction modulation of light *IEEE J. Quant. Electron.* **26** 1234
[161] Maker G T and Ferguson A I 1990 Ti:Sapphire laser pumped by a frequency-doubled diode-pumped Nd:YLF laser *Opt. Lett.* **15** 375

[162] Malcolm G P A and Ferguson A I 1991 Ti:sapphire laser pumped by a frequency-doubled diode pumped Nd:YLF laser *Opt. Commun.* **82** 299
[163] Basu S and Byer R L 1988 Continuous-wave mode-locked Nd:glass laser pumped by a laser diode *Opt. Lett.* **13** 458
[164] Dimmick T E 1990 Semiconductor-laser-pumped CW mode-locked Nd:phosphate glass laser oscillator and regenerative amplifier *Opt. Lett.* **15** 177
[165] Krausz F, Turi L, Brabec T, Kuti Cs, Wintner E and Schmidt A J 1990 Mode locking of a diode laser pumped Nd:glass laser by regenerative feedback *Tech. Dig. CLEO'90 (Anaheim, CA)* Paper CFR6
[166] Zhou F and Ferguson A I 1990 Tunable single frequency operation of a diode laser pumped Nd:YAG microchip at 1.3 μm *Electron. Lett.* **26** 490
[167] Zhou F and Ferguson A I 1991 Frequency stabilization of a diode-laser-pumped microchip Nd:YAG laser *Opt. Lett.* **16** 79
[168] Storm M E and Rohrbach W W 1989 Single-longitudinal-mode lasing of Ho:Tm:YAG at 2.091 μm *Appl. Opt.* **28** 4965
[169] Storm M E, Koch G J and Rohrbach W W 1990 Single-mode lasing of Ho:Tm:YAG at 2.091 μm in a monolithic crystal *Tech. Dig. ASSL'90 (Salt Lake City, Utah)* Paper WA3
[170] Storm M E 1991 Spectral performance of monolithic holmium and thulium lasers *Tech. Dig. ASSL'91 (Hilton Head, SC)* Paper TuB2
[171] Zhou B, Kane T J, Dixon G J and Byer R L 1985 Efficient, frequency-stable laser-diode-pumped Nd:YAG laser *Opt. Lett.* **10** 62
[172] Owyoung A, Hadley G R, Esherick P, Schmitt R L and Rahn L A 1989 Gain switching of a monolithic single-frequency laser-diode-excited Nd:YAG laser *Opt. Lett.* **10** 484
[173] Scheps R and Heller D F 1989 Single-mode operation of a standing wave Nd laser pumped by laser diodes *Appl. Opt.* **28** 5288
[174] Otsuka K and Kubodera K 1980 Effects of high density pumping on relaxation oscillations and mode spectra in lasers *IEEE J. Quant. Electron.* **16** 419
[175] Shoemaker D, Brillet A, NaryMan C, Cregut O and Kerr G 1989 Frequency-stabilized laser-diode-pumped Nd:YAG laser *Opt. Lett.* **14** 609
[176] Nachman P, Munch J and Yee R 1990 Diode-pumped, frequency-stable, tunable continuous-wave Nd:glass laser *IEEE J. Quant. Electron.* **26** 317
[177] Henderson S W and Hale C P 1990 Tunable single-longitudinal-mode diode laser pumped Tm:Ho:YAG laser *Appl. Opt.* **29** 1716
[178] Scheps R and Myers J 1990 A single frequency Nd:YAG ring laser pumped by laser diodes *IEEE J. Quant. Electron.* **26** 413
[179] Clarkson W A and Hanna D C 1989 Single frequency Q-switched operation of a laser diode-pumped, Nd:YAG ring laser *Opt. Commun.* **73** 469
[180] Kane T J and Byer R L 1985 Monolithic, unidirectional single-mode Nd:YAG ring laser *Opt. Lett.* **10** 65
[181] Cheng E A P and Kane T J 1991 High power single-mode diode-pumped Nd:YAG laser using a monolithic nonplanar ring resonator *Opt. Lett.* **16** 478
[182] Trutna W R Jr, Donald D K and Nazarathy M 1987 Unidirectional diode-laser-pumped Nd:YAG ring laser with a small magnetic field *Opt. Lett.* **12** 248
[183] Kane T J, Nilsson A C and Byer R L 1987 Frequency stability and offset locking of a laser-diode-pumped Nd:YAG monolithic nonplanar ring oscillator *Opt. Lett.* **12** 175
[184] Bush S P, Gungor A and Davis C C 1988 Studies of the coherence properties of a diode pumped Nd:YAG ring laser *Appl. Phys. Lett.* **53** 646
[185] Day T, Gustafson E K and Byer R L 1990 Active frequency stabilization of a 1.062 μm, Nd:GGG diode-laser-pumped nonplanar ring oscillator to less than 3 Hz of relative linewidth *Opt. Lett.* **15** 221
[186] Bromley L J and Hanna D C 1991 Single frequency Q-switched operation of a diode-laser pumped Nd:YAG ring laser using an acousto-optic modulator *Opt. Lett.* **16** 378
[187] Clarkson W A and Hanna D C 1991 Acousto-optically induced unidirectional single mode operation of a Q-switched miniature Nd:YAG ring laser *Opt. Commun.* **81** 375
[188] Clarkson W A and Hanna D C 1991 Single frequency Q-switched operation of a diode pumped Nd:YLF ring laser *Opt. Commun.* **84** 51
[189] Evtuhov V and Siegman A E 1965 A 'twisted mode' technique for obtaining axially uniform energy density in a laser cavity *Appl. Opt.* **4** 142
[190] Wallmeroth K 1990 Monolithic integrated Nd:YAG laser *Opt. Lett.* **15** 903
[191] Wallmeroth K and Peuser P 1988 High power, CW, single-frequency TEM_{00}, diode-laser-pumped Nd:YAG laser *Electron. Lett.* **24** 1086
[192] Hughes D W, Phillips M W, Barr J R M and Hanna D C 1992 A laser diode pumped Nd:glass laser:modelocked, high power and single frequency performance *IEEE J. Quant. Electron.* **28** To be published
[193] McCarthy M J and Hanna D C 1992 Continuous wave modelocked singly resonant optical parametric oscillator synchronously pumped by a laser diode pumped Nd:YLF laser *Opt. Lett.* To be published